Vipp1 structure and function
in cyanobacteria and chloroplasts

Dissertation

zur Erlangung des Doktorgrades der Fakultät für Biologie

der Ludwig-Maximilians-Universität München

Vorgelegt von

Elena Aseeva

München

14.11.2005

Contents:

Abbreviations

BCIP	5-bromo-4-chloro-3-indolyl phosphate
BN-PAGE	Blue-Native PAGE
BSA	bovine serum albumin
α-CT	acetyl-CoA carboxyltransferase α-subunit
Cytf	cytochrome f
DM	n-Decyl-β-D-maltoside
hcf	*high chlorophyll fluorescence*
Hsp70	heat shock protein of 70 kDa
LHC	light harvesting complex
LHCB	light harvesting complex of photosystem II
NBT	nitra blue tetrazolium
PCR	polymerase chain reaction
PMSF	phenylmethylsulfonyl fluoride
PSI	photosystem I
PSII	photosystem II
Psa	photosystem I subunit
Psb	photosystem II subunit
PspA	phage shock protein A
RT	room temperature
SDS-PAGE	SDS-polyacrylamyd gel electrophoresis
Tic	translocon of the inner envelope of chloroplast
Toc	translocon of the outer envelope of chloroplast
v/v	volume per volume
Vipp1	vesicle inducing protein in plastids 1
w/v	weight per volume

1. Abstract

The vesicle inducing protein in plastids 1 (Vipp1) is an essential factor for the development and maintenance of the thylakoid membrane. Depletion of Vipp1 in both *Arabidopsis* and *Synechocystis* mutants severely affects their ability to form thylakoids and consequently to perform photosynthesis. This work focuses on structural and functional properties of Vipp1. It was shown that Vipp1 assembles into a homooligomeric complex of ca. 2000 kDa. The presence of the Vipp1 complex was detected in cyanobacteria, green algae and higher plants, thereby identifying oligomerization as an essential feature for the function of Vipp1. A detailed computer analysis of Vipp1 secondary structure in different organisms revealed functionally important characteristics of the protein and allowed to discern specific features of its C-terminal domain. Based on the structural analysis, biochemical characterization of Vipp1 domains was carried out. It appeared that the PspA-like domain of Vipp1 is responsible for both complex formation and localisation of Vipp1 at the inner envelope of chloroplasts while the C-terminal domain is not involved in these processes. In order to closer elucidate the function of Vipp1, an analysis of *Arabidopsis* plants with moderate deficiency in Vipp1 protein level was performed. From results obtained in this analysis it can be proposed that Vipp1 acts at the initial stages of thylakoid biogenesis. Oligomerization of Vipp1 appeared to be a prerequisite for the process of thylakoid formation to commence. Moreover, the extent of thylakoid membrane formation is directly correlated to the amount of Vipp1 protein available in the chloroplast.

2. Zusammenfassung

Das Vipp1 (vesicle inducing protein in plastids 1) Protein ist eine essentielle Komponente der Thylakoidbiogenese in Cyanobakterien und Chloroplasten. Eine signifikante Reduzierung des Gehalts an Vipp1 sowohl in *Arabidopsis* als auch *Synechocystis* führt zu einem fast vollständigen Verlust an Thylakoiden und damit zur Beeinträchtigung der Photosynthese. Der Schwerpunkt dieser Arbeit war die Untersuchung struktureller und funktionaler Eigenschaften des Vipp1 Proteins. Es konnte gezeigt werden, dass Vipp1 homooligomere Komplexe von ca. 2000 kDa bildet. Diese Komplexe wurden in Cyanobakterien, Grünalgen und höheren Pflanzen gefunden. Dies legt nahe, dass die Oligomerisierung eine wesentliche Eigenschaft der Funktion von Vipp1 darstellt. Eine detaillierte Analyse der Sekundärstruktur verschiedener Vipp1 Proteine ermöglichte die Identifizierung funktional wichtiger Charakteristika von Vipp1, sowie spezifischer Eigenschaften der C-terminalen Domäne. Basierend auf diesen strukturellen Daten wurden biochemische Untersuchungen der Vipp1 Domänen durchgeführt. Diese ergaben, dass die PspA-ähnliche Domäne für die Komplexbildung und die Lokalisierung des Proteins an der inneren Hüllmembran von Chloroplasten notwendig ist. Im Gegensatz dazu spielt die C-terminale Domäne für diese Prozesse keine Rolle. Weiterführende funktionelle Untersuchungen an *Arabidopsis* Pflanzen mit einer nur teilweisen Verringerung des Vipp1-Gehaltes ergaben, dass Vipp1 in den frühen Stadien der Thylakoidbiogenese fungiert. Eine Mindestmenge an Vipp1 scheint dabei für die Oligomerisierung des Proteins notwendig zu sein, welche wiederum eine Voraussetzung dafür ist, dass die Thylakoidbiogenese einsetzt. Danach korreliert die weitere Ausbildung der Thylakoidmembran mit der Menge von Vipp1, die diesem Prozess zur Verfügung steht.

3. Introduction

3.1. Evolution of oxygenic photosynthesis

Oxygenic photosynthesis, i.e. the conversion of light energy into chemical energy accompanied by CO_2-fixation and oxygen release, is an important characteristic of plants and cyanobacteria. Oxygenic photosynthesis developed from a simpler anoxygenic, or non-oxygen-evolving form of photosynthesis, in which bacteria use reduced molecules such as H_2, H_2S, S and small organic molecules as an electron source to generate NADH and NADPH with the help of a single photosystem (Xiong and Bauer, 2002). The appearance of oxygenic photosynthesis, utilizing two photosystems working in tandem together with the oxygen evolving complex, allowed for the efficient usage of water as a source of electrons, producing oxygen as a by-product. The oxygen generated during photosynthesis is the source of virtually all oxygen in the atmosphere and thus enabled life on earth in its present form.

According to current knowledge, oxygenic photosynthesis first evolved in the ancestor of present-day cyanobacteria (Xiong et al., 2000). In the course of evolution the ability to perform oxygenic photosynthesis was passed on to the eukaryotic cell in a singular endosymbiotic event, in which an ancestral cyanobacterium was engulfed by a heterotrophic host cell (Margulis, 1970; Moreira et al., 2000; Palmer, 2000). This resulted in the appearance of a new organelle, the chloroplast, and enabled the host cell to exploit the energy of oxygenic photosynthesis for its needs. Beside photosynthesis, a number of other metabolic processes, indispensable for the cell, take place in the chloroplast. These include the biosynthesis of amino acids, fatty acids and porphyrines as well as sulphate and nitrite reduction.

A great part of chloroplast genes have been transferred to the nucleus in the course of evolution (Martin et al., 1998). Thereby, the host cell took control over the biological processes taking place in the cyanelle. Only about 5-10% of the chloroplast proteins are now organelle-encoded. They generally include a number of key components of the photosynthetic apparatus as well as a major part of the chloroplasts transcription and translation machinery. Therefore, the regulation of chloroplast development is very complex and requires a tight coordination between the nuclear and plastid genomes. Cyanobacteria, as the evolutionary progenitor of chloroplasts, propagate by simple divisions. In a similar fashion, the chloroplasts of most algae are distributed into the

daughter cells. In land plants, chloroplasts develop from a non-differentiated plastid type, the proplastid (Mühletaler and Frey-Wyssing, 1959). This organelle contains only very few residual membranes, lacking a structured thylakoid membrane system. Indeed, plastids represent a whole organelle family, including several non-photosynthetic forms, namely amylo-, leuko-, chromo- and etioplasts, a feature, which cannot be attributed to the cyanobacterial ancestor. Instead, these plastid forms must be the result of a newly generated developmental program. Moreover, plastids do not only differentiate into specialized types but also posses a remarkable capacity for interconversion.

A very important evolutional acquisition of organisms performing oxygenic photosynthesis is the thylakoid system, the site of location of their photosynthetic machinery. The development of thylakoids strongly correlates with the occurrence of oxygenic photosynthesis, and almost all organisms performing this process posses this specialized membrane system. Whereas the nature of the photosynthetic reaction and the principle architecture of the thylakoid membrane are by now reasonably well understood, many aspects of the evolution and progression of thylakoid biogenesis remain elusive. Despite a detailed structural and biochemical characterization of the thylakoid membrane, our knowledge about the molecular processes involved in its formation and maintenance remains unsatisfactory.

3.2. Structure and composition of the thylakoid membrane

The thylakoid membrane system of cyanobacteria as well as of many algae is built up of long lamellae that enclose an aqueous compartment, the lumen. This relatively simple organisation becomes more complex in the course of evolution. The first signs of thylakoid differentiation appear in green algae (Stefansson et al., 1997; Bhattacharya and Medlin, 1998). This process further continues in mosses, which already posses a thylakoid structure similar to that of higher plants. The thylakoid membrane of higher plants is subdivided into grana stacks and stroma lamellae, which connect the granas. Such architecture allows the chloroplast to significantly increase the surface utilized for the photosynthetic process and thereby to achieve a more efficient exploitation of light energy. Moreover, the compartmentalization and flexibility of the thylakoid system allows for a finer regulation.

There are four major protein complexes embedded into the thylakoid membrane: photosystem I and II (PSI and PSII, respectively) with their antenna proteins, the cytochrome b_6f complex and the ATP synthase. They include a variety of co-factors and

pigments, and require multiple assembly steps. Moreover, the photosynthetic complexes are not equally distributed along the thylakoid membrane but have preferential locations. PSI and ATP synthase are more abundant in stroma lamellae while PSII and LHCII are predominantly found inside the grana stacks (Andersson and Anderson, 1980; van Roon et al., 2000). The cytochrome b_6f complex is most likely equally distributed (Albertsson, 2001; Allen and Forsberg, 2001), although there is no general agreement on this question (Vallon et al., 1991; van Roon et al., 2000). The spatial separation of photosynthetic components may serve as a means of fine-tuning the photosynthetic process (Horton, 1999). Taking into consideration a faster excitation energy trapping in PSI, separate location of both photosystems may prevent an uncontrollable spill-over of the excitation energy from PSII to PSI (Trissl and Wilheim, 1993). It may also help in balancing between the linear and the cyclic electron transfer (Joliot and Joliot, 2002; Joliot et al., 2004). The stacking provides PSII with large functional antennae and facilitates regulation of the light requirement for photosynthesis (Anderson et al., 1986; Dekker and Boekema, 2005). Moreover, the distribution of photosynthetic membrane components changes in response to short- and long-term adaptation stimuli (Allen, 1992; Depege et al., 2003; Bellafiore et al, 2005; Walters, 2005).

Thylakoids have an unusual lipid composition, which is similar in cyanobacteria and higher plants (Dilley et al., 2001; Kelly and Dormann, 2004). Their main components are unsaturated galactolipids, namely monogalactosyl diacylglycerol (MGDG), which makes up more then 50% of the total thylakoid lipids, and digalactosyl diacylglycerol DGDG (about 25%). Additionally, the thylakoids contain phosphatidylglycerol and sulfoquinovosyl diacylglycerol together with other minor components. The protein to lipid ratio in the thylakoid membrane is very high (Block et al., 1983). Moreover, the distribution of the lipids in the thylakoid membrane is not equal in the leaflets facing lumen and the stroma, which is probably important for the function of the thylakoids (Douce et al., 1996).

3.3. Formation of the thylakoid membrane

Little is known about the initial steps of thylakoid development during the maturation of chloroplasts from undifferentiated proplastids. In the presence of light proplastids develop into chloroplasts, and the thylakoid system has to be built up more or less *de novo*. The development seems to begin by invagination of the inner envelope (Muehletaler and

Frey-Wyssing, 1959). These invaginations give rise to lamellar structures that are afterwards complemented by disc-shaped grana stacks. The formation of the thylakoid lipid bilayer is tightly coupled to the accumulation of photosynthetic protein components. These proteins play a role in stabilizing the newly evolving membrane, about half of which is constituted by non-bilayer forming lipids. It was shown that the association of purified MGDG (which is known to form an inverted hexagonal phase in an aqueous solution) with LHCII resulted in the formation of ordered lamellae structures (Simidjiev et al., 2000).

Some of the photosynthetic components are believed to be inserted into the inner envelope before being transferred to the thylakoids. It is proposed that in *Chlamydomonas* the insertion of LHCs is coupled to chlorophyll biosynthesis and occurs at the inner envelope (Hoober and Eggink, 2001). Similarly, cytokinin-stimulated synthesis and accumulation of the ATP synthase in the inner envelope was shown for etioplasts of *Lupinus luteus* (Sherameti et al., 2004). Interestingly, a number of photosynthetic proteins in fully assembled state were also found in the plasma membrane of *Synechocystis*, implying their possible involvement in the initial steps of the cyanobacterial thylakoid biogenesis (Zak et al., 2001; Huang et al., 2002). It is important to notice that a surprisingly large set of the photosynthetic proteins, such as the subunit F_0II of the ATP synthase and subunits W and X of the PSII reaction center, are believed to use a spontaneous mechanism for membrane insertion (Michl et al., 1994; Kim et al., 1998; Kim et al., 1999), which can be considered as a means of rapid initiation of thylakoid membrane formation at the stage when thylakoid protein transport pathways have not yet been assembled. Moreover, some of the thylakoid membrane proteins cannot be assigned to any of the identified thylakoid protein transport pathways. They either require yet unidentified assistance factors or the inner envelope as an intermediate location for their insertion (Fincher et al., 2003). Interestingly, several key components of the translocation machineries, such as SecY and TatC, belong to this group of proteins (Fincher et al., 2003; Mant and Robinson, 2005).

During early stages of chloroplast development, a physical link can be observed between the inner envelope and the evolving thylakoid membrane (Muehletaler and Frey-Wyssing, 1959; Hoober et al., 1991). Once the thylakoids have matured, this connection seems to be lost. This raises the question of how the biogenesis of mature thylakoid membrane is maintained. It is still controversial how the lipids, synthesised at the envelope, are delivered to thylakoids. One cannot exclude the presence of temporary

connections between the thylakoids and the inner envelope. Another possible way to transport the lipids would be trafficking by vesicles. Vesicle flow was observed between the inner envelope and the thylakoid membrane of chloroplasts in several higher plants as well as in some ferns and mosses (Westphal et al., 2001b; Westphal et al., 2003). A closer look at this phenomenon revealed that its features are similar to the vesicle traffic in yeast homotypic vacuole fusion (Westphal et al., 2001b). While vesicular transport is a feature common to all eukaryotic organisms, the vesicle flow between chloroplast membranes is the only known example of such a system utilized by a life form of a prokaryotic origin. It is also possible that, beside lipids, other components of the thylakoid membrane that are synthesized at the envelope or have to cross it *en route* to the thylakoids could be transported by the vesicle system. Hydrophobic components would be especially likely candidates to take an advantage of a system that allows avoiding contact with the aqueous stroma environment (Vothknecht and Westhoff, 2001).

3.4. Vipp1 is an ubiquitous component of thylakoid biogenesis

One of the components shown to be important for thylakoid development and maintenance is the <u>v</u>esicle <u>i</u>nducing <u>p</u>rotein in <u>p</u>lastids 1 (Vipp1). Vipp1 (original name IM30) was first identified as a protein targeted to chloroplasts, which is synthesised as a 37 kDa precursor and processed to the mature form with a molecular mass of 30 kDa (Li et al., 1994). Vipp1 was originally found associated with both the inner envelope and thylakoid membrane of *Pisum sativum*. In contrast, in the cyanobacterium *Synechocystis* Vipp1 was identified only in the plasma membrane (Westphal et al., 2001a). Interestingly, despite the fact that Vipp1 is found associated with membrane fractions, hydropathy analysis shows that it should be a soluble protein (Li et al., 1994; Westphal et al., 2001a). Further structural analysis performed on the Vipp1 from pea revealed its strong tendency to form α-helices throughout the entire polypeptide as well as two potential coiled-coil regions (Li et al., 1994).

First indications that Vipp1 plays a role in thylakoid biogenesis came from an analysis of the *hcf155* (Δ*vipp1*) mutant of *Arabidopsis*, which contained a T-DNA insertion in the promoter region of the *vipp1* gene (Kroll et al., 2001). The mutation resulted in a more then 80% reduction of the Vipp1 protein content. Such plants were only able to grow heterotrophically and exhibited an *albino* phenotype. Interestingly, the lack of pigmentation became especially apparent with ageing of the plants, and the colour of

leaves displayed a change from pale green to almost white in the course of growth. The *high chlorophyll fluorescence* phenotype, observed for Δ*vipp1* is often a characteristic of mutants with an impaired photosynthetic electron transport chain. Indeed, the spectroscopic analysis of Δ*vipp1* plants revealed a general dysfunction of their photosynthetic apparatus. Electron microscopy showed that the thylakoid system of mutant plants is severely distorted and mostly consists of unstructured lamellae and some membranous inclusions. Moreover, the vesicle flow, typically observed between the inner envelope and the thylakoid membrane of chloroplasts, was absent in the Δ*vipp1* plants (Kroll et al., 2001). This phenotype pointed toward a role of Vipp1 in the process of thylakoid formation.

Disruption of the *VIPP1* gene in *Synechocystis* further confirmed this assumption, since it also caused an almost complete loss of the thylakoid system in the mutant (Westphal et al., 2001a). Remarkably, the complete segregation of Δ*vipp1 Synechocystis* cells could not be achieved. This, together with the fact that no *vipp1* knock-out has been identified for *Arabidopsis*, indicates that at least minor amounts of Vipp1 are necessary to maintain the viability of these organisms, and the complete absence of Vipp1 would be lethal. Moreover, the similarity of phenotypes caused by Vipp1 depletion in the higher plant *Arabidopsis* and cyanobacterium *Synechocystis* implies that the role of Vipp1 in the thylakoid biogenesis is evolutionary conserved.

Recent advances in genome sequencing made it possible to obtain information about Vipp1 and its homologues in a wide range of organisms. The analysis of fully sequenced genomes showed that genes encoding Vipp1 proteins are found in almost all organisms performing oxygenic photosynthesis. Moreover, homologues of Vipp1 can be found in many bacteria in form of the phage shock protein PspA. Vipp1 of *Pisum sativum* has 31% identity and 53% similarity with PspA from *E. coli* (Li et al., 1994) and both proteins share the highly α-helical structure. The most apparent difference between Vipp1 and PspA is the presence of an additional C-terminal extension of about 30 amino acids found in all Vipp1 proteins. Phylogenetic analysis indicated that the *VIPP1* gene originated from *PSPA* by a gene duplication and was then passed on from the cyanobacterial endosymbiont to the plant genome (Westphal et al., 2001a). Whereas cyanobacteria mostly posses both *PSPA* and *VIPP1*, the *PSPA* gene seems to have been eliminated in plants.

The similarity of both proteins could imply a redundancy of their functions. This, however, is ruled out by the phenotype of the *Synechocystis vipp1* mutant, which displays a severe defect of the thylakoid system despite the presence of a functional *PSPA* gene in its

genome. Moreover, the fact that Vipp1 is found exclusively and ubiquitously in organisms performing oxygenic photosynthesis, i.e. in organisms possessing thylakoid membranes, implies special importance of this protein in the generation of the thylakoid system. In this respect, the additional C-terminal extension of Vipp1 is of particular interest, as a distinctive feature of all Vipp1 proteins. Due its similarity to PspA, Vipp1 can be regarded as a PspA-like protein with a specific C-terminal domain. The generation of this domain is in direct connection with the novel function of the PspA homologue in thylakoid biogenesis.

3.5. Phage shock protein A (PspA) of bacteria

Despite a detailed phenotypic analysis of the Δ*vipp1* mutant, the function of Vipp1 in the thylakoid biogenesis remains elusive. Considerable progress was, however, made in the investigation of its bacterial homologue, PspA. A significant structural similarity of both proteins suggests that even though their functions are different, they might be based on similar principles of action. Thus, the current knowledge about PspA might provide a basis for the understanding of Vipp1 function.

PspA is a protein that is produced in bacterial cells under various stress conditions and plays a critical role in maintaining membrane integrity. Filamentous phage infection (Brissette et al., 1990), inhibition of lipid biosynthesis (Bergler et al., 1994) and misinsertion or blockage of the protein export machinery (Kleerebezem and Tommassen, 1993; Hardie et al., 1996; Kleerebezem et al., 1996; Jones et al., 2003; DeLisa et al., 2004) are among the stimuli triggering *PSPA* induction. More general stress conditions, such as heat and osmotic shock (Brissette, 1990), exposure to organic solvents (Kobayashi et al., 1998) and ionophores (Weiner and Model, 1994) have also been reported to induce *PSPA* expression. All of these stresses can be linked to the dissipation of the proton motive force (PMF), and there is mounting evidence that PspA is crucial for the maintenance of the PMF over the bacterial membrane. Consistently, Δ*pspA* mutants of *E. coli* appeared to be incapable of sustaining the PMF under stress conditions (Kleerebezem and Tommassen, 1993).

The involvement of PspA in the regulation of bacterial protein import has first been studied for the general secretory pathway (Sec pathway). It was shown that the blocking of the bacterial Sec translocation with excess of a prePhoE precursor leads to *PSPA* induction

(Kleerebezem and Tommassen, 1993). Moreover, enhanced PspA level was also observed in conditional mutants of several Sec components (Kleerebezem and Tommassen, 1993).

The discovery of SRP, Tat and YidC-dependent translocation systems in bacteria posed the question whether PspA is involved in their regulation as well. In this regard, it was recently shown that the depletion of YidC results in enhanced PspA level (van der Laan et al., 2003; Jones et al., 2003). YidC plays a dual role in translocation by working either in cooperation with the Sec translocase or independently, and has a direct effect on the insertion of a Sec machinery component, SecE, as well as on the insertion of subunits a and c of the F_0 part of F_0F_1 ATPase and cytochrome o oxidase (Yi et al., 2003). Depletion of YidC was shown to be accompanied by dissipation of the proton motive force (van der Laan et al., 2003). This is most probably due to defects in the assembly of cytochrome o oxidase and F_0F_1 ATPase, since the insertion of the purified F_0 c-subunit into YidC-containing inner membrane vesicles was shown to be PMF-independent (van der Laan, 2004). Thus, the primary reason for *PSPA* induction under these conditions remains to be elucidated.

In a recent work of DeLisa and colleges, it was shown that the overexpression of PspA from a multi-copy plasmid relieved saturation of the Tat pathway and increased the translocation rate of the heterologous TorA-GFP-SsrA and the native Tat substrates SufI and CueO (DeLisa et al., 2004). Consistently, deletion of the *PSPA* gene affected the translocation of the TorA-GFP-SsrA. These results imply a possible regulating role for PspA in a Tat-dependent bacterial translocation. However, the data concerning PspA expression in *tat* mutants are contradictory (DeLisa et al., 2004, Jones et al., 2003) and it is not clear if defects in Tat pathway lead to the PspA induction.

Interestingly, no involvement of PspA in SRP-dependent translocation could be shown, and the mutations in all SRP components did not result in an induction of *PSPA* (Jones et al., 2003). It is important to notice that mutations in the SRP affect only the presentation of substrates to the Sec translocon. Therefore, these results are consistent with the observation made in studies of *sec* mutants that the entry of a precursor into the translocation pore, i.e. conditions potentially leading to a PMF dissipation, is necessary to induce PspA synthesis (Kleerebezem and Tommassen, 1993). All in all, PspA rather seems to help in the protection of membrane integrity *per se* than to be involved in specific steps of protein translocation.

The *PSPA* gene is part of the *pspABCDE* operon, which is conserved in many Gram-negative bacteria. Transcription of the *pspABCDE* operon is initiated from a promoter located upstream of the *PSPA* gene by σ54-dependent RNA polymerase (Brissette et al., 1991). The *PSPF* gene, which is located upstream of the *pspABCDE* operon and transcribed in the opposite direction, encodes an activator of the *psp* operon (Jovanovic et al., 1996). PspF binds to sites overlapping its own promoter, thereby simultaneously regulating its own expression (Weiner et al., 1995; Jovanovic and Model, 1997). In addition to PspF, other proteins appear to influence the transcription of the *psp* operon. PspA was shown to serve as a negative regulator of PspF (Dworkin et al., 1999; Elderkin et al., 2002; Elderkin et al., 2005). The PspB and PspC proteins were shown to act cooperatively as positive regulators of the *psp* operon, possibly by relieving the PspA-mediated repression (Weiner et al., 1991; Weiner and Model, 1994). Recently, one more member of the *PSPF* regulon, PspG, was identified (Lloyd et al., 2004). Expression of *PSPG* is activated by PspF and negatively regulated by PspA (Lloyd et al., 2004; Green and Darwin, 2004). The exact function of PspG, as well as of PspD and PspE proteins so far remains unclear. Intriguingly, no homologues of the *psp* operon proteins, except PspA, have been identified in cyanobacteria.

In *E. coli* cells PspA is found both in a soluble form as well as associated with the inner membrane (Brissette et al., 1990; Kleerebezem and Tommassen, 1993), and shuttling between the cytoplasm and the inner membrane presumably reflects different functional states of the protein (Adams et al., 2003). Recently, PspA was shown to assemble into an oligomeric complex with an estimated molecular mass of 1023 kDa (Hankamer et al., 2004). The rotationally symmetric PspA ring consists of nine subunits, each containing four PspA molecules, and has the outer diameter of 200 Å. PspA complex assembly and disassembly is believed to modulate PspA activity via a number of protein/protein interactions. Firstly, it has been shown that in the assembled state the PspA complex completely inhibits the activity of PspF, which is the transcriptional activator of PspA. The membrane-associated function of PspA is modulated via its interactions with the transmembrane proteins PspB and PspC (Model et al., 1997; Adams et al., 2003). According to the current model (Hankamer et al., 2004), alteration in the membrane stability and dissipation of the proton motive force leads to the disassociation of PspC homodimers in the inner membrane and promotes its interaction with PspB. The PspC/PspB complex preferentially binds to oligomerized PspA shifting it to a membrane-

associated form. This, in turn, inhibits the interaction of PspA with PspF resulting in enhanced PspA synthesis.

It remains enigmatic how exactly PspA protects the membrane. The large size of the PspA complex leads to the supposition that, being recruited to a "damaged" membrane, PspA-complex attaches to it and seals the damaged region, thereby somehow maintaining membrane integrity under stress conditions. Yet, this assumption needs to be experimentally confirmed. It is also unclear how the change in membrane stability is sensed by the proteins of the *psp* operon, and the primary signal for PspA-dependent membrane protection still has to be identified. Moreover, although organisation in the *psp* operon has been shown for a wide range of gram-negative bacteria (Darwin, 2005), in other bacterial systems, such as cyanobacteria, most of the *PSP* genes appear to be lost and *PSPA* represents the only known component of the *psp* response.

The evolution of oxygenic photosynthesis, which is correlated with the appearance of the thylakoid membrane as a structural platform for this process, necessitated the development of a PspA-like protein with a novel function, Vipp1. Despite its evident importance for the formation of the thylakoid system, the exact function of Vipp1 so far remains elusive. The aim of the present work was a detailed characterization of structural and functional properties of Vipp1 in order to provide an insight into the role it plays in biogenesis of the thylakoid system in cyanobacteria and plants.

4. Materials

4.1. Chemicals

All chemicals were purchased from Sigma Aldrich (München, Germany), Roth (Karsruhe, Germany) and Merck (Darmstadt, Germany). Bis[Sulfosuccinimidyl]suberate (BS^3) was from Pierce (Bonn, Germany) and n-Decyl-β-D-maltoside (DM) was from Glycon GmbH (Luckenwalde, Germany). Nitrocellulose membrane was purchased from Protran (Schleicher&Schuell, Germany), Ni-NTA Superflow column was from Qiagen (Hilden, Germany), and Superose 6 HR 10/300 was from Amersham biosciences (Freiburg, Germany).

4.2. Enzymes and kits

Restriction enzymes were purchased from Fermentas (St. Leon-Rot, Germany) and T4-DNA ligase was purchased from Eppendorf (Hamburg, Germany). For plasmid DNA isolation in a small scale FastPlasmid[TM] Mini (Eppendorf, Hamburg, Germany) was used. Large scale DNA isolation was performed with Nucleobond[R] AX (Macherey-Nagel (Düren, Germany). In-gel purification of DNA-fragments was made using Nucleospin[R] Extract II (Macherey-Nagel (Düren, Germany).

4.3. Primers

For Vipp1-GFP and Vipp1-RFP:

V-forward	5'-ggactagtatggctctcaaagcttca-3'
V-reverse	5'-cggggtacccaaagtcgttagctttc-3'
Vm-reverse	5'-ggggtaccccaattctttcttcaag-3'

For α-Vcterm antibody:

V-C-forward	5'-ggagagcttcctcctggaaga-3'
V-C-reverse	5'-ttaaagctcctttgatctttttct-3'

For 6xHis-Vipp1:

Vipp1gate-f-st	5'-ggggacaagtttgtacaaaaaagcaggctctatgaatcttttttgaacgattttgtag-3'
Vipp1gate-rev-stop	5'-ggggaccactttgtacaagaaagctgggtcctaaaagtcgttagctttccttcgc-3'

For analysis of VIPP1-PROTA plants:

Gene specific primers for the wild type *VIPP1* gene

At155-RB3   5'-cttgaagctatcactgagatgcgcc-3'

At155-LB4rev   5'-gttctgagaggggaatcctgagg-3'

T-DNA specific primer

LBTAG14   5'-ggtaataggacactgggattcgtc-3'

CaMV-35S specific primer

35-S2   5'-gtaagggatgacgcacaatcc-3'

All primers were purchased from MWG-Biotech AG (Ebersberg, Germany).

4.4. Vectors

pOL-LP (GFP) (gift from Dr. J. Meurer)

pOL-RFP (gift from Dr. J. Meurer)

pCR T7/NT-TOPO (Invitrogen GmbH, Germany)

pDEST17 (Invitrogen GmbH, Germany)

4.5. *E. coli* strains

JM-109   New England Biolabs (Frankfurt, Germany)

BL21(DE3)lysS   Novagen (Madison, USA)

Top10   Invitrogen (Karsruhe, Germany)

4.6. Antibodies

The primary antibodies α-LHCB, α-PsbP, α-Tic110, α-Tic32, α-Tic40, α-Tic55, α-Tic62, α-Toc75, α-Vipp1 were raised against heterologously expressed full-length protein of *Pisum sativum*. α-Vcterm, α-α-CT and α-HCF136 were raised against *Arabidopsis* polypeptides. α-PspA was raised against heterologously expressed full-length protein of *E. coli*. α-AtpB, α-AtpC, α-AtpH, α-AtpG, α-AtpF, α-PsbO, α-PsaD, α-PsbD and α-Cytf were raised against *Chlamydomonas* or spinach polypeptides. α-PsbP was raised in chicken and all other antisera were raised in rabbit.

4.8. Plant material and growth conditions

Seedlings of *Arabidopsis thaliana* were grown either on soil or on MS-plates (Murashige and Skoog, 1962) supplemented with 1% (w/v) sucrose as described before (Kroll et al., 2001). In both cases the plants were grown in a climate chamber at 20°C with a 14 h/10 h daylight cycle at a photon flux density of 20 µmol photons m^{-2} s^{-1}. Prior to illumination, plates were placed for 2 days at 4 °C to induce germination. Propagation of both Δ*vipp1* and Vipp1-ProtA plants occurred via heterozygous offspring. All comparisons between mutant and wild type plants were carried out with leaf material of the same developmental stage.

Pisum sativum (sort "Arvica", Praha, Czech Republik) was grown on soil under day-night cycle (12 h of light) in a climate chamber, at 20°C.

4.9. *Synechocystis* growth conditions

Synechocystis sp. PCC 6803 liquid culture was grown in BG11 medium (Ono and Murata, 1981) under continuous light (30-40µEm^{-2}, s^{-1}) at 30°C for 3-4 days.

5. Methods

5.1. Molecular biological methods

5.1.1. Polymerase Chain Reaction (PCR)

DNA fragments for cloning into plasmid vectors were generated by the polymerase chain reaction (PCR) (Saiki et al., 1988). The restriction sites for cloning were integrated in the primers used for PCR. *Arabidopsis* cDNA library was used as template. PCR reaction was carried out as recommended by polymerase supplier (TripleMaster PCR System, Eppendorf, Hamburg, Germany).

5.1.2. Cloning techniques

Plasmid DNA isolation, restriction of plasmid DNA and PCR-amplified fragments, as well as agarose gel electrophoresis were carried out according to standard procedures (Sambrook et al., 1989). Standard techniques were applied for ligation of pVipp1 and pVipp1m into pOL-LP vector. Vipp1Δα-helix-GFP was created by restriction of pVipp1-GFP with Eco72I at positions 475 bp and 637 bp followed by re-ligation of the plasmid. pVipp1-RFP was created by subcloning *vipp1* into pOL-LP where the GFP sequence was replaced with RFP (Mollier et al., 2002). Cloning of *VIPP1* from *Arabidopsis* into pCR T7/NT-TOPO and pDEST-17 (Invitrogen GmbH, Germany) was performed according to

Table 1: List of constructs used in this study. The name (column 1), the vector used for cloning (column 2), the biological source (column 3) and the purpose of cloning (column 4) are given for each construct.

Construct	Vector	Organism	Purpose
pVipp1-GFP	pOL-LP	*Arabidopsis thaliana*	protoplast transformation
pVipp1-RFP	pOL-RFP	*Arabidopsis thaliana*	protoplast transformation
pVipp1m-GFP	pOL-LP	*Arabidopsis thaliana*	protoplast transformation
pVipp1Δα-helix-GFP	pOL-LP	*Arabidopsis thaliana*	protoplast transformation
6xHis-Vipp1	pDEST17	*Arabidopsis thaliana*	expression
Vcterm	pCR T7/NT-TOPO	*Pisum sativum*	expression

manufacturer's recommendations. To create Vcterm, base pairs 915-1041 of *VIPP1* gene from *Pisum sativum* amplified by PCR were cloned into the pCR T7/NT-TOPO. All constructs used in this study (Table 1) were verified by sequencing (Sequence laboratories, Göttingen, Germany).

5.2. Biochemical methods

5.2.1. Determination of chlorophyll concentration

Determination of chlorophyll concentrations in higher plants was carried out as described by Arnon (1949). For *Synechocystis,* the method of Williams (1988) was used.

5.2.2. Determination of protein concentration

Concentration of total protein in *E. coli* cells expressing 6xHis-Vipp1 was determined by Bio-Rad Protein Essay Kit (Bio-Rad Laboratories GmbH, Munich, Germany).

5.2.3. SDS-polyacrylamid electrophoresis (SDS-PAGE) and Western-blotting

The electrophoretical separation of proteins in denaturing polyacrylamid gels was carried out according to the method of Laemmli (1970). Separating gels with polyacrylamid concentration ranging from 8% to 15% were used. Before being applied to the gel, proteins were solubilized in sample buffer (Laemmli-buffer) and incubated for 2 min at 95 C°. Gels were stained either by Coomassie Brilliant Blue R250 or silver stained as described (Sambrook et al., 1989).

For immunodetection, proteins were transferred onto a nitrocellulose membrane in a "semi-dry-blot" apparatus (Amersham Pharmacia Biotech, Freiburg) as described (Towbin et al., 1979). Nitrocellulose with bound proteins was first incubated for 30 min in blocking buffer (100 mM Tris-HCl, pH 7.5, 150 mM NaCl, 0.3% skim milk powder, 0.03% BSA, 0,1% Tween-20) and then with primary antibody diluted in blocking buffer (the dilution varied with the choice of antibody) for 1.5 h – 2 h at RT or overnight at 4°C. Non-bound antiserum was removed from the membrane by 3x15 min wash in wash buffer (100 mM Tris-HCl, pH 7.5, 150 mM NaCl, 0.1% Tween-20). The choice of secondary antibody depended on the method of visualization.

For colorimetric reaction with alkaline phosphatase substrate, the secondary antibody (anti-rabbit or anti-chicken alkaline phosphatase conjugate) was applied to the membrane for 1 h. After the excess of antibody was removed from the membrane (3x15 min in wash

buffer) immunoreaction was visualized by incubation with 100 mM Tris-HCl, pH 9.5, 100mM NaCl, 5M MgCl$_2$, 0.035% NBT (w/v), 0.0175% BCIP (w/v).

For chemiluminescent method of protein detection (ECL), HRP-conjugated goat anti-rabbit antibody was used as secondary antibody. Proteins were visualized with ECL Advanced ^{TM} Western Blot Detection Kit (Amersham Biosciences, Freiburg, Germany).

5.2.4. Blue-Native electrophoresis (BN-PAGE)

Blue-Native polyacrylamid gel electrophoresis (BN-PAGE) was carried out on 3%-13% gradient gels, basically according to the method of Schägger and von Jagow (1991) for separation of native protein complexes. Fractions corresponding to 50 µg chlorophyll for chloroplasts, 10 µg chlorophyll for *Synechocystis* and 100 µg of total protein for *E. coli* were used per 1 cm wide gel lane. In case of Vipp1-ProtA and Δ*vipp1* plants analysis, chlorophyll concentration was determined for wild type and the amounts of fresh leaf tissue corresponding to 50 µg/ml in the wild type were taken for each sample.

The samples were solubilized in 60 µl buffer containing 750 mM aminocaproic acid, 50 mM Bis-Tris pH 7.0, 0.5 mM EDTA-Na$_2$ and incubated for 3-5 min on ice. n-Decyl-β-D-maltoside (DM) was added to a final concentration of 1% and samples were incubated on ice for further 10 min. After a 10 min centrifugation at 4°C and 21000xg the supernatant was collected and loading buffer (5% Serva Blue G, 750 mM aminocaproic acid) was added to 1/10 of the sample volume.

5.2.5. Isolation of intact chloroplasts from *Arabidopsis thaliana*

Arabidopsis chloroplasts were isolated from 3-4 week old plants grown in a climate chamber at 20°C under constant light. The leaves were grinded in *isolation buffer* (50 mM Tris-HCl, pH 8.0, 20 mM EDTA, 0.33 M Sorbitol, 14.3 mM β-mercaptoethanol) and suspension was filtered through mull and 25 µm gauze. Chloroplasts were collected after centrifugation (3 min at 3500 rpm, 4°C) and purified on 40%-80% Percoll gradient (9000 rpm for 15 min, 4°C). Intact chloroplasts were collected from 80% interface, washed twice with *isolation buffer* and centrifuged at 3500 rpm for 4 min. All procedures were carried out on ice.

5.2.6. Isolation of intact chloroplasts from *Pisum sativum*

Intact chloroplasts were isolated from the leaves of 10-12 day old garden pea. The plants were grown on soil under day-night cycle (12 h of light) in a climate chamber, at 20°C. Isolation of chloroplasts was performed as described in Bölter et al. (1998).

5.2.7. Isolation of inner envelope from chloroplasts of *Pisum sativum*

Chloroplast inner envelope membranes from pea were purified according to the method of Keegstra and Yousif (1986) modified by Waegemann and Soll (1995).

5.2.8. Isolation of *Synechocystis* membranes

Logarithmic-growth phase culture (OD_{750}=0.7-0.8) was harvested by centrifugation (3000 rpm, 15 min, 4°C). Cells were washed with *Buffer A* (50 mM Hepes-NaOH, 0.5 M sucrose, 15 mM NaCl, 5 mM $MgCl_2$, pH 7.0) and pelleted again. Cells were broken by vortexing with glass beads (120 - 210 micron, Sigma) in *Buffer A*. Glass beads were used in the ratio 1:2 to the sample volume. The sample was vortexed 3 times for 2 min each, with 1 min incubation on ice between each vortex. Unbroken cells were removed by brief centrifugation (4000xg for 5 min at 4°C). Membranes were sedimented by centrifugation at 22000 rpm for 30 min at 4°C and washed twice in *BufferA*.

5.2.9. Isolation of total membranes of *Chlamidomonas reinhardtii*

The *Chlamidomonas reinhardtii* wild-type strain 137c was grown on Tris-acetated medium (Gorman and Levine, 1965) at 25°C and 40 μE $m^{-2}s^{-1}$ to the cell density of $2x10^6$ cell/ml. Membrane extraction was performed as described in Ossenbühl et al., 2004.

5.2.10. Preparation of *Echerichia coli* total lysate

E. coli cells were collected by centrifugation at 6000xg for 5 min. The pellet was resuspended in 50 mM Hepes-KOH, pH 7.6 and sonicated 3 times for 15 sec. The sample was supplemented with Laemmli-buffer and incubated for 2 min at 95 °C.

5.2.11. Preparation of thylakoid membranes from wild type, K2 and Δ*vipp1* *Arabidopsis* plants

Several leaves of 3-4 week old heterotrophically grown *Arabidopsis* plants were weighed out and equal amount of material was used for each preparation. The leaves were

grinded with mortar and pestle in TMK buffer (10 mM Tris-HCl, 10 mM $MgCl_2$, 20 mM KCl, pH 6.8), filtered through 25 μm gauze and the filtrate was centrifuged at 6000 rpm in a table top centrifuge for 10 min.

5.2.12. Cross-linking of pea inner envelope proteins with Bis[Sulfosuccinimidyl]suberate (BS³)

Isolated inner envelope membranes were resuspended in 50 mM Hepes-KOH, pH 7.6 and incubated with non-membrane permeable cross-linker Bis[Sulfosuccinimidyl]suberate (BS³). Total protein concentration in each sample was 0.2 μg/μl. BS³ was added to the final concentration of 0.5 mM. Samples were incubated on ice or at room temperature for different periods of time, from 5 min to 1 h. The reaction was stopped by the addition of 10 mM Tris, pH 7.5. Proteins were separated on 12.5% SDS-PAGE and analyzed by Western blot analysis using α-Vipp1 and α−Vcterm antisera.

5.2.13. Trypsin-digest

Inner envelope membrane of pea (approx. 3 μg/μl of total protein) and total *E. coli* membranes were incubated with different concentrations of trypsin (3.3 μg/ml, 10 μg/ml and 20 μg/ml) at 25°C for 90 s in buffer containing 50 mM Hepes, 5 mM $CaCl_2$. To stop the reaction, PMSF was added to 10 mM and the samples were incubated for 10 min on ice. Proteins were subsequently separated on 12.5% SDS-PAGE and analyzed by Western Blotting using α−Vipp1, α−Vcterm, α-PspA antisera.

5.2.14. Media for protoplast isolation and transformation

F-PCN medium

Murashige and Skoog (MS) mineral salts (as in Gamborg B5 medium (Gamborg et al., 1998)), supplemented with PC-vitamins (200 mg/l Myo-inositol, 1.0 mg/l thiamin-HCl, 2.0 mg/l Ca-panthotenat, 2.0 mg/l nicotine acid, 2.0 mg/l pyridoxin-HCl, 0.02 mg/l biotin), 1.0 mg/l 6-benzylaminopurin (BAP), 0.1 mg/l α-naphtaleneacetic acid (NAA), 20 mM MES, pH 5.8 (KOH) and 80 g/l glucose. Osmomolarity was adjusted to 550 mOsm with glucose.

F-PIN medium

MS mineral salts and PC-vitamins like for F-PCN medium, 20 mM MES, pH 5.8 (KOH) and 130 g/l sucrose. Osmomolarity was adjusted to 550 mOsm with sucrose.

Transformation medium

15 mM $MgCl_2x6H_2O$, 0.1% MES, 0.5 M mannitol, pH 5.8 (KOH). Osmolarity was adjusted to 550 mOsm with mannitol.

40% PEG

40% PEG 1500, 70 mM $Ca(NO_3)_2$, 550 mM mannitol, pH 9.75 (KOH)

5.2.15. Isolation of protoplasts from tobacco leaves

Transient transformation of tobacco protoplasts with constructs carrying GFP- or RFP-tags was carried out according to the modified method of Koop et al (1996). Seedlings of *Nicotiana tabacum* cv. petite Havana were germinated on B5-modified medium (Gamborg et al., 1976) and leaves of 3-4 week old plants were used in all experiments. The leaves were cut with a razor blade in 0.1 cm wide stripes and incubated with 0.5% cellulase and 0.5% macerase in F-PIN medium for 12-14 h. Resulting suspension was filtered through 100 µM gauze. The gradient for separating intact protoplasts was created by overlaying F-PCN medium on the filtered suspension. After centrifugation at 70xg for 10 min intact protoplasts were collected from the interface between F-PIN and F-PCN mediums, washed with *transformation medium* and sedimented at 50xg for 10 min. Protoplasts were counted in Fuchs-Rosenthal counting chamber and cell density was adjusted to $5x10^6$ protoplasts/ml. 50 µg of DNA was used for one transformation. When same aliquot of protoplasts was transformed with two different constructs (co-transformation), 25 µg of each DNA was used. 25 µl of DNA (2 µg/µl DNA in 10 mM Tris-HCl, 1mM EDTA, pH 5.6) was put to 100 µl of protoplasts in a 30 mm Petri dish and gently mixed by shaking, after which the suspension was supplemented with 125 µl of 40% PEG, gently mixed again and incubated for 7.5 min. This followed by adding 125 µl of F-PCN medium and incubation for two further minutes. Protoplasts were diluted with 2.5 ml of F-PCN medium and incubated in dark at 25°C. Specific GFP- and RFP-fluorescence could be observed between 24 h and 72 h after transformation.

5.2.16. Isolation of protoplasts from *Arabidopsis* leaves

Leaves of 3-4 week old *Arabidopsis* plants grown on soil were cut up into small pieces with a sharp razor blade in 10 ml of buffer containing F-PIN supplied with 0,1 g cellulase, 0,03 g mazerase and 10% BSA. The leaves were transferred into 100 ml flasks, infiltrated under vacuum for ca. 30 sec and incubated in dark for ca. 90 min with agitation (40 rpm). Protoplasts were released from the leaf tissue by centrifugation at 80 rpm for 1 min. Further steps were performed as in **5.2.15.**

5.2.17. Isolation of chloroplasts from tobacco protoplasts

$2x10^6$ protoplasts transformed with GFP- or RFP-fusion constructs were collected by centrifugation at 100xg for 10 min and resuspended in *isolation medium* (330 mM Sorbit, 20 mM MOPS, 13 mM Tris-HCl, pH 7.9, 1 mM $MgCl_2$, 0,02% BSA, 1 mM β-mercaptoethanol, 0.1 mM PMSF). Cells were lysed on ice for 30 minutes and chloroplasts were isolated by filtering the suspension through 25 μm gauze.

5.2.18. Heterologous protein expression

Protein overexpression was carried out in *E. coli* strain BL21(DE3)lysS. Transformed with a corresponding construct bacteria were incubated at 37°C in LB-medium supplemented with antibiotics ampicillin and chloramphenicol for selection (Sambrook et al., 1989). Cells were grown to the mid-log phase (OD_{550}=0.5-0.8) after which the protein was expressed by induction with 0.4 mM IPTG during 2 h to 4 h at 37°C.

5.2.19. Protein purification and production of polyclonal antibody

α-Vcterm antiserum was prepared against the C-terminal 42 amino acids of the pea Vipp1 protein. Corresponding DNA sequence was cloned into the pCR T7/NT-TOPO expression vector (Invitrogen, Karlsruhe, Germany), which carries an N-terminal 6xHis tag. Heterologously expressed protein was purified on a Ni-NTA Superflow column (Qiagen, Hilden, Germany) under denaturing conditions following the manufacturer's instruction. Antisera were made by injection of purified protein into rabbit by Pineda antibody service (Waldbronn, Germany).

5.2.20. Purification of Vipp1 complex under native conditions

E. coli cells overexpressing Vipp1-6xHis were collected after centrifugation at 8000xg for 10 minutes, resuspended in *lysis buffer* (100 mM Tris-HCl, pH 7.6; 50 mM NaCl, 75 mM NaSCN) and lysed using a French press cell. The suspension was centrifuged at 15000xg for 10 minutes, the pellet was resuspended in *lysis buffer* supplemented with 1.1% CHAPS, 600 mM NaCl and incubated for 2 h at 4°C with agitation, followed by a centrifugation for 1 h at 15000xg. The supernatant, containing solubilized proteins, was applied onto a Ni-NTA column (Qiagen, Hilden, Germany) in binding buffer (50 mM Hepes-KOH, pH 7.6, 300 mM NaCl, 10 mM imidazole, 75 mM NaSCN, 0.05% CHAPS) and Vipp1-6xHis was purified under native conditions according to the manufacturer's instructions with the exception that 75 mM NaSCN was added to washing and elution buffer. Eluted Vipp1 was centrifuged for 10 min at 21000xg and analysed on Superose 6 HR 10/300 column.

5.2.21. Purification of Vipp1 complex under denaturing conditions with subsequent renaturation

E. coli cells overexpressing Vipp1-6xHis were harvested by centrifugation at 8000xg for 10 min, resuspended in 50 mM Hepes-KOH, pH 7.6 and lysed by passage through a French pressure cell. The suspension was centrifuged at 15000xg for 10 min, the pellet was resuspended in *urea buffer* (4 M urea, 50 mM NaCl, 50 mM NaH_2PO_4, 10 mM Hepes, 5 mM Tris-HCl, pH 8.0) and incubated for 20 min at RT with agitation. Non-solubilized and aggregated protein was removed by centrifugation (10 min, 15000xg, 4°C). Protein concentration was estimated and adjusted to 20 mg/mg with *urea buffer*, then the supernatant was diluted 1:20 (v/v) in *renaturation buffer* (55 mM Tris-HCl, pH 8.2, 10.56 mM NaCl, 0,44 mM KCl, 0.055% PEG 3350, 550 mM guanidine-HCl, 1.1 mM EDTA, 440 mM sucrose, 1 mM DTT, 0.3 mM DM) to yield a final concentration of 1 mg/ml protein and incubated for 14 h at 4° with rotating. The sample was centrifuged at 15000 g for 10 min to remove aggregated proteins. The supernatant was dialysed against 20 mM Hepes-KOH, pH 7.6, 50 mM NaCl, 300 µM PMSF and centrifuged again (21000xg, 10 min, 4°) before being applied to the Superose 6 10/300.

5.2.22. Size-exclusion chromatography

Size-exclusion chromatography was performed on Superose 6 HR 10/300 column (Amersham biosciences, Freiburg, Germany) with FPLC system (Amersham biosciences, Freiburg, Germany).

For the examination of the Vipp1-complex purified under native conditions, the column was equilibrated with 20 mM Tris-HCl, pH 7.6, 50 mM NaCl, 75 mM NaSCN. Vipp1 purified under denaturing-renaturing conditions was analyzed on the column equilibrated with 20 mM Hepes-KOH, pH 7.6, 50 mM NaCl. The column was calibrated with the following molecular weight markers: blue dextran (2000 kDa), catalase (232 kDa), aldolase (158 kDa), bovine serum albumin (67 kDa) and chymotrypsinogen (25 kDa) in the appropriate buffer. Size exclusion was performed with a flow rate of 0.3 ml/min. Fractions (0.25 ml) were collected and analyzed by Western blotting with α-Vipp1 antiserum.

5.3. Fluorometric and absorption studies

5.3.1. Measurement of chlorophyll fluorescence emission at 77K

For 77K fluorescence spectroscopy, equal amounts of wild type, K2 and Δ*vipp1* leaf tissue (fresh weight) were ground with a mortal and pestle in *isolation buffer* (330 mM sorbitol, 50 mM Tris-HCl, pH 8.0, 20 mM EDTA, 14.3 mM β-mercaptoethanol). The samples were subsequently filtered through a single layer of gauze. In case of wild type and K2, the samples were adjusted to equal chlorophyll concentration. For Δ*vipp1*, the amount of fresh leaf material equal to wild type was used. The samples were diluted with *isolation buffer*, transferred into glass capillaries, and instantly frozen in liquid nitrogen. The analysis was performed with a LS55 luminescence spectrometer using FL Winlab software (Perkin-Elmer, Buckinghamshire, UK) and an excitation light with a wavelength of $\lambda = 430$ nm.

5.3.2. Chlorophyll *a* fluorescence measurements

Chlorophyll *a* fluorescence was measured using a commercial pulse amplitude modulated fluorometer PAM 101 interfaced with the PAM data acquisition system PDA-100 (Walz, Effeltrich, Germany). Unless noted otherwise, the detection was performed at 20°C. Leaves were dark-adapted for 5 min prior to the fluorescence induction. The fluorescence induction kinetics were performed on the same leaves with increasing red

actinic illumination (650 nm light) with intensities of 40, 80 and 120 $\mu E/m^2s$, which corresponds to 3.5, 16.8 and 76.0 μmol photons m^{-2} s^{-1}. The intensity of saturating light flashes (800 ms) used for detection of the maximal fluorescence yield (Fm) and the maximal fluorescence during induction (Fm') was 4000 μmol photons m^{-2} s^{-1}. Saturating pulses determining Fm' were given at intervals of 20 sec. F_0 indicates the minimal fluorescence yield of dark-adapted plants. The variable fluorescence (Fv) was calculated as (Fm - Fo), and the ratio Fv/Fm reflects the potential yield of the photochemical reaction of PSII (Krause and Weis, 1991). Non-photochemical quenching (NPQ) was determined as described (van Kooten and Snel, 1990).

Photosystem I activity induced by far-red light (720 nm) was measured at 830 nm. Plants were pre-illuminated with actinic light before the saturating white light pulse was applied. After the signal dropped back to the original level, actinic light was switched off to monitor P700 reduction, and subsequently far-red light was applied to oxidize P700. A saturating pulse was then given in order to re-reduce P700. The far-red light was switched off, followed by a flash of saturating light. The redox level of PSI was determined as $\Delta A/\Delta A_{max}$ as described (Klughammer and Schreiber, 1993).

5.4. Electron microscopy

5.4.1. Transmission electron microscopy

Pieces of leaf tissue were fixed immediately with 2.5% glutardialdehyde in fixative buffer (75 mM sodium cacodylate, 2 mM $MgCl_2$, pH 7.0) for 1 h at room temperature; rinsed several times in fixative buffer and post-fixed for 2 h with 1% osmium tetroxide in fixative buffer at room temperature. After two washing steps in distilled water, the cells were stained *en bloc* with 1% uranyl acetate in 20% acetone for 30 min. Dehydration was performed with a graded acetone series. Samples were infiltrated and embedded in Spurr's low-viscosity resin (Spurr, 1969). After polymerisation, ultra thin sections with a thickness between 50 and 70 nm were cut with a diamond knife and mounted on uncoated copper grids. The sections were post-stained with aqueous lead citrate (100 mM, pH 13.0). All micrographs were taken with an EM 912 electron microscope (Zeiss, Oberkochen, Germany) equipped with an integrated OMEGA energy filter operated in the zero loss mode.

5.4.2. Negative stain electron microscopy

Samples for EM were prepared using the conventional negative staining procedure. One drop of purified Vipp1-complex diluted 1:10 was placed onto a carbon-coated grid hydrophylized by charge glow. After 2 min the protein solution was removed and the grid was dried on air. Grids spread with Vipp1-complex were treated for 1 min with 1% uranyl acetate and 0.01% glucose in water, briefly rinsed with a drop of water and then air dried. The samples were examined with a ZEISS EM 912 transmission electron microscope operated with the OMEGA energy filter in the zero-loss mode.

All electron microscopy was performed in collaboration with Prof. Dr. G. Wanner.

5.5. Imaging

All fluorescence images were obtained by an epi-fluorescence microscope (polychrome IV System, Till Photonics GmbH, Munich, Germany) using GFP, FITC, and rhodamin filter sets. Pictures were taken with a cooled IR CCD camera and visualized by the TILLvision 4.0 software.

5.6. Secondary structure analysis

Secondary structure prediction was performed using NPS@ (Network Protein Sequence Analysis, France) (Combet et al., 2000) and Jnet (Cuff and Barton, 2000).

6. Results

6.1. Analysis of the secondary structure of Vipp1 and PspA proteins

Initial analysis of Vipp1 and PspA suggested a strong conservation in their secondary structure. To accurately identify and characterize the features common to these proteins, a detailed secondary structure prediction was performed.

Analysis of the secondary structure of Vipp1 and PspA proteins was carried out by using two methods: NPS@ (Network Protein Sequence Analysis, France) (Combet et al., 2000), which makes consensus predictions by analysing the results of eight different programs (DPM, DSC, GOR4, HNN, PHD, Predator, SIMPA96 and SORM), and JPRED, where the neural network program Jnet is used for the prediction (Cuff and Barton, 2000).

An initial analysis was performed on Vipp1 of *Arabidopsis thaliana*. The cleavable presequence of Vipp1 was not considered and the Vipp1 amino acid sequence was analysed from the start of the mature protein indicated as amino acid one in figure 1. NPS@ results show that from amino acid position 1 to 216 Vipp1 has eight α-helices interrupted by short random coil regions of up to six amino acids (Fig. 1). The region from amino acid 217 to 243 represents the only comparatively long non-helical region of the protein, namely a random coil. This region is followed by an additional α-helix comprised of 14 amino acids (Fig.1). The results obtained by JPRED analysis principally agree with NPS@ with the exception that a random coil between amino acids 82 and 85 is not detected with the JPRED program.
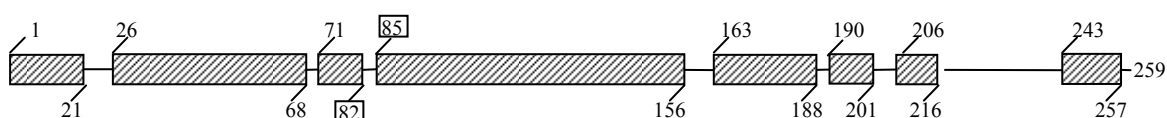

Figure 1: Secondary structure prediction of the Vipp1 protein of *Arabidopsis thaliana*.

Dashed rectangles represent α- helical regions; lines represent unstructured coil regions. Numbers correspond to the number of the first (above) and the last (below) amino acid of each α-helix. Underlined numbers indicate a random coil region predicted only by NPS@ and not by JPRED. Representation of both α-helices and random coil regions is in due proportion to the length of Vipp1. Amino acid 1 is the start of the mature protein.

To elucidate whether the secondary structure of Vipp1 and PspA is conserved, a structure comparison was performed for several different Vipp1 and PspA proteins by both NPS@ and JPRED programs. This analysis revealed a strong structural conservation of all PspA and Vipp1 proteins. It is furthermore evident that the whole of PspA and the PspA-like part of Vipp1 show principally identical features (Fig. 2). Both consist of several α-
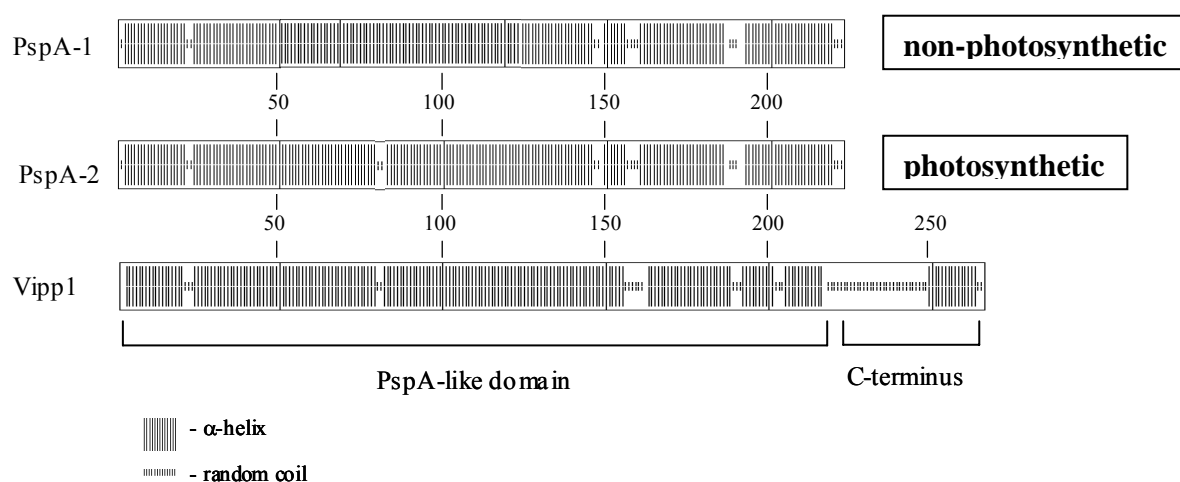

Figure 2: Secondary structure analysis of PspA and Vipp1 proteins.
Model of the secondary structure of consensus sequences of PspA and Vipp1 proteins as predicted by NPS@. PspA-1 and PspA-2 represent two alternative secondary structure models of PspA proteins derived from the analysis. Designations of α-helical and random coil regions are given in the picture. Numbers correspond to the number of amino acids in the sequence.

helices interrupted by short unstructured regions. The position of the helices is very similar to those described above for *Arabidopsis*. Only slight shifts in the positioning of the α-helices (two to three amino acids) are observed between different organisms. This shift can be explained by the differences in their amino acid sequences and does not principally change the described structure.

However, a detailed comparison of the PspA proteins from non-photosynthetic and photosynthetic organisms revealed one difference in the secondary structure of these two groups. According to the NPS@ approach, PspA proteins of *Escherichia coli, Bacillus subtilus, Methanosarcina acetivorans* and *Shewanella oneidensis* contain a single long α-

28

helix from amino acid 21 to amino acid 156-158, while in PspA of the cyanobacteria *Synechocystis* sp*., Nostoc (Anabaena)* sp., *Thermosynechocystis elongatus* and the photosynthetic α-proteobacterium *Rhodospirillum robrum* this helix is interrupted by a short random coil approx. at position 80. This feature is also shared by all Vipp1 proteins (see Fig. 2). The detection of the long α-helical region in PspA proteins of the first group is in agreement with the fact that they also show a higher tendency to form α-helical coiled-coil structures in this region, when analysed by the COILS program (data not shown). At the same time, JPRED always predicts a short random coil region at position 80, thereby splitting the long α- helix into two. This may be due the fact that JPRED uses a neural network to make predictions and is trained on a common set of proteins possessing α-helices not longer than 40 to 60 amino acids. This can lead to the automatic disruption of the extra-long α-helical region predicted by NPS@. Assuming that the structure predicted by NPS@ is correct, the random coil structure at the position 80 is a later acquisition of PspA proteins in photosynthetic bacteria that was subsequently passed on to Vipp1. On the other hand, we cannot exclude that the prediction of a 130 amino acid long α-helix in bacterial PspA proteins might be an artefact provided by the NPS@ program. This question remains disputable.

Of special consideration is a C-terminal extension of variable length that was shown to be characteristic for Vipp1 in the preliminary analysis. Despite considerable differences in the amino acid sequence, the C-terminal domain of all Vipp1 proteins analysed shows principally identical features on the level of secondary structure (see Fig. 2). The domain comprises a random coil followed by a short α-helix. The size of the random coil region may vary between different species ranging from 17 amino acids (*Nostoc punctiforme*) to 32 amino acids (*Synechocystis* sp.), and it is the major determinant of differences in total amino acid length of Vipp1 proteins. However, the observed structure was found in all Vipp1 proteins analysed. The conservative nature of the secondary structure of the C-terminal domain indicates that its specific features are necessary for the function of Vipp1. The analysis of many Vipp1 and PspA proteins showed, nevertheless, that the length of the proteins is not a sufficient criterion to differentiate between Vipp1 and PspA, since some organisms have PspA proteins with a prolonged C-terminus or even posses two PspA-like proteins of similar length. This situation is exemplified in figure 3 for two strains of *Nostoc*. Assuming that the secondary structure of the C-terminus is important for the
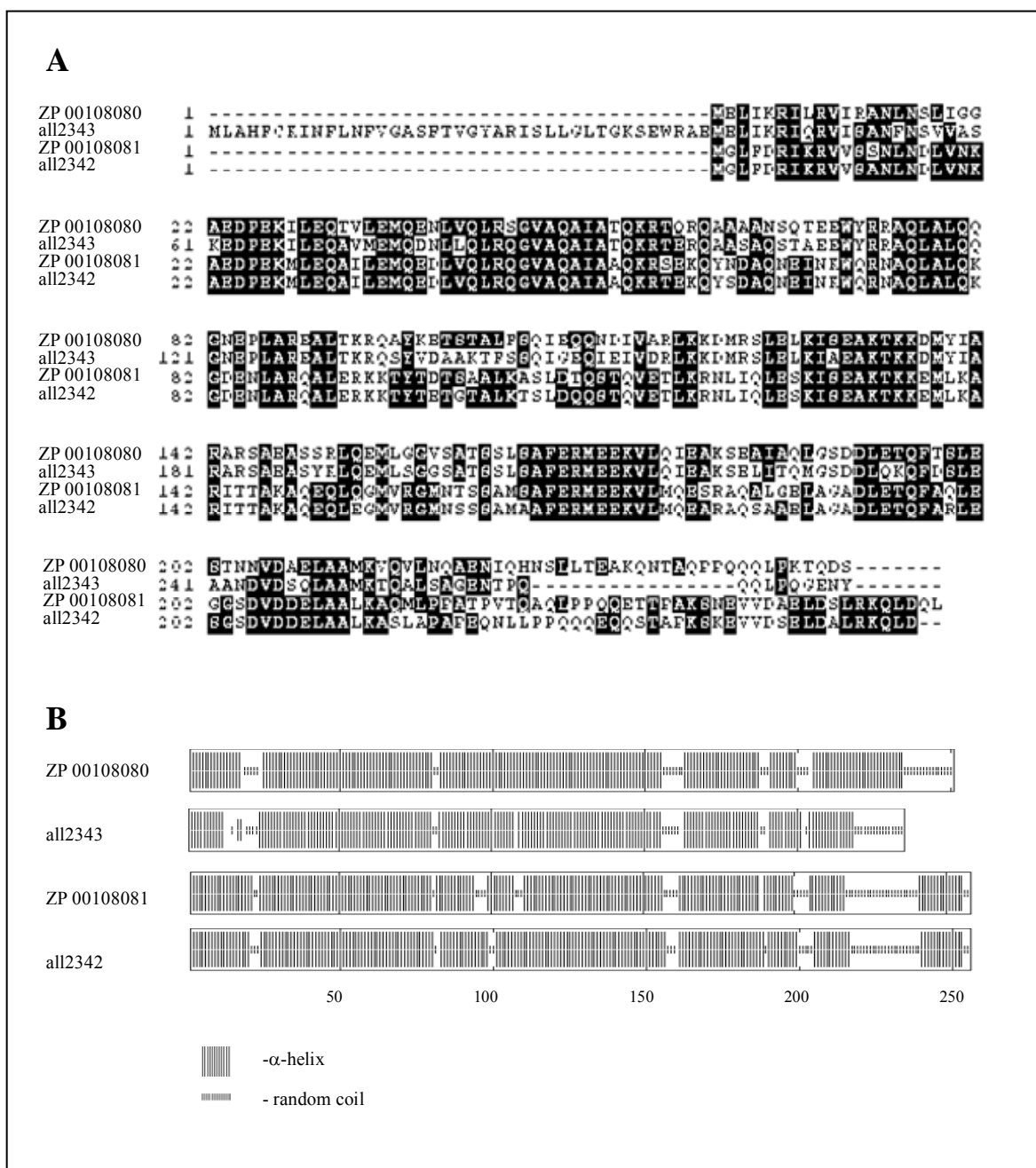
A

B

Figure 3: Sequence comparison and secondary structure comparison of PspA-like proteins of *Nostoc*.
(A) Sequence comparison of ZP 00108080 and ZP 00108081 of *Nostoc punctiforme* PCC 731 and all2342 and all2343 of *Nostoc* sp. PCC 7120. The alignment was performed using the program ClustalW 1.7. Identical amino acids are underlined in black using BOXSHADE. (B) Secondary structure comparison of ZP 00108080, ZP 00108081, all2342 and all2343. Designation of α-helical and random coil regions is given in the picture. Numbers correspond to numbers of amino acids in the sequence.

function of Vipp1, it may be used it as a decisive factor to discern true Vipp1-proteins from PspA. This assumption was tested in the analysis of the PspA-like proteins of the two

Nostoc strains: *Nostoc punctiforme* PCC 731 and *Nostoc* sp. PCC 7120. Each of these species posses two proteins found in a BLAST search as homologues of PspA. In both cases the genes encoding these proteins are located next to each other (ZP 00108080 and ZP 00108081 for *Nostoc punctiforme*, all2342 and all2343 for *Nostoc* sp. PCC 7120). ZP 00108080, ZP 00108081 and all2342 have a size of about 250 amino acids, which is approx. 30 amino acids longer then the PspA of *E. coli*. The 274 amino acid long all2343 shows an additional N-terminal extension of 39 amino acids (Fig. 3). This extension is likely due to incorrect genome annotation since none of the other known Vipp1 or PspA proteins possess a similar region. Therefore, the first 39 amino acids of all2343 are not taken into consideration in the following analysis. The alignment of the four proteins showed that ZP 00108081 has higher similarity to all2342 (91% vs. 70% similarity to ZP 00108080 and all2343) while ZP 00108080 is more similar to all2343 (80% vs. 70% similarity to ZP 00108081 and all2342). Moreover, ZP 00108081 and all2342 share a conserved region in their C-terminal parts (Fig. 3 A). Therefore, it is likely that ZP 00108080 and all2343, as well as ZP 00108080 and all2342 are evolutionary closer related to each other. This, however, does not provide information whether they belong to the group of Vipp1 or PspA proteins. In order to distinguish between PspA and Vipp1 proteins of *Nostoc punctiforme* and *Nostoc* sp. PCC 7120, a secondary structure comparison was performed as described above. The analysis revealed that ZP 00108081 and all2342 both posses a C-terminal region with features characteristic for Vipp1, namely a random coil followed by a short C-terminal α−helix.

In contrast, the C-termini of ZP 00108080 and all2343 exhibit a different secondary structure. The C-terminus of all2343 exhibits only a random coil structure, while in the case of ZP 00108080 the last α-helix of the Psp-like domain is prolonged and is followed by a random coil without creating an α-helical structure at the end of the protein. From this feature it appears that ZP 00108080 and all2343 belong to the group of PspA proteins. While the structural analysis appears conclusive, this assumption requires experimental support.

Whereas this example illustrates that the length and the level of amino acid similarity in PspA-like proteins may differ, Vipp1 can most likely be distinguished from PspA due to the specific secondary structure of its C-terminal domain. This approach was used further to differentiate between PspA and Vipp1 proteins in various groups of organisms. The result is summarized in table 2. It supports the notion that PspA is present in diverse

groups of non-photosynthetic and photosynthetic bacteria. In contrast, Vipp1 was identified in most organisms performing oxygenic photosynthesis, from cyanobacteria to higher plants, with the exception of *Gloebacter violaceus*. Interestingly, both *Prochlorococcus marinus* MIT9313 and *Synechococcus* sp. WH 8102 seem to have lost the gene coding for PspA and thus posses only Vipp1. It is therefore tempting to speculate that already at this stage of evolution of oxygenic photosynthesis PspA might have become dispensable.

Table 2: Distribution of PspA and Vipp1 proteins between different organisms. The analysed proteins (column 1) were assigned to the PspA or Vipp1 group according to their predicted secondary structure (columns 2 and 3, respectively). The gene names are given in the case of fully annotated genome, otherwise accession numbers are given.

	PspA	Vipp1
Escherichia coli	BAA14873	-
Bacillus subtilus str. 168	NP 388499	-
Shewanella oneidensis MR-1	NP 717415	-
Yersinia pestis	NP 993471	-
Vibrio cholerae O1 biovar eltor str. N16961	NP 231314	-
Methanosarcina acetivorans C2A	NP 616394	-
Rhodospirillum rubrum	ZP 00269524	-
Prochlorococcus marinus MIT9313	-	PMT1361
Nostoc sp. PCC 7120	all2343	all2342
Nostoc punctiforme	ZP 00108080	ZP 00108081
Synechococcus sp. WH 8102	-	SYNW1879
Thermosynechococcus elongatus	tll1692	tlr0283
Synechococcus elongatus PCC 6301	YP 171452	YP 171453
Synechocystis sp. PCC 6803	slr1188	sll0617
Gloeobacter violaceus PCC 7421	grl0898	-
Chlamydomonas reinhardtii	-	AAU06582
Arabidopsis thaliana	-	AT1G65260
Pisum sativum	-	Q03943
Zea mais	-	AY105003
Oryza sativa	-	BAB90216

As mentioned above, the amino acid sequence of the Vipp1 C-terminus can vary greatly. Nevertheless, it does display certain characteristic features. One of such features is the presence of a leucin and one or two conservative prolins (LP or LPP, Fig. 4, asterisk) in the beginning of the random coil region. These residues are also found in several PspA proteins, very close to the end of the protein (Fig. 4).
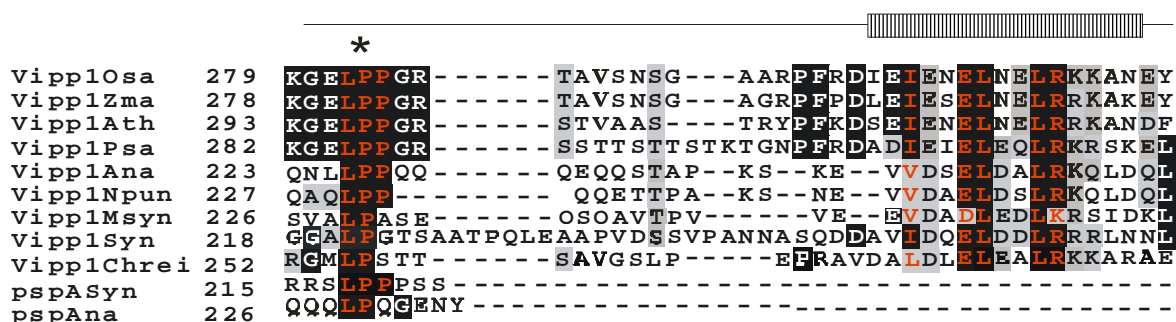
```
              *
Vipp1Osa   279  KGELPPGR------TAVSNSG---AARPFRDIEIENELNELRRKKANEY
Vipp1Zma   278  KGELPPGR------TAVSNSG---AGRPFPDLEIESELNELRRKAKEY
Vipp1Ath   293  KGELPPGR------STVAAS----TRYPFKDSEIENELNELRRKANDF
Vipp1Psa   282  KGELPPGR-----SSTTSTTSTKTGNPFRDADIEIELEQLRKRSKEL
Vipp1Ana   223  QNLLPPQQ------QEQQSTAP--KS--KE--VVDSELDALRKQLDQL
Vipp1Npun  227  QAQLPP--------QQETTPA--KS--NE--VVDAELDSLRKQLDQL
Vipp1Msyn  226  SVALPASE------OSOAVTPV------VE--EVDADLEDLKRSIDKL
Vipp1Syn   218  GGALPGTSAATPQLEAAPVDSSVPANNASQDDAVIDQELDDLRRRLNNL
Vipp1Chrei 252  RGMLPSTT-----SAVGSLP-----EPRAVDALDLELEALRKKARAE
pspASyn    215  RRSLPPPSS------------------------------------
pspAna     226  QQQLPQGENY----------------------------------
```

Figure 4: Sequence comparison of the C-terminal domain of different Vipp1 proteins.

C-termini of Vipp1 of *Oryza sativa* (Osa), *Zea mais* (Zma), *Arabidopsis thaliana* (Ath), *Pisum sativum* (Psa), *Nostoc* (*Anabaena*) sp. (Ana), *Nostoc punctiforme* (Npun), *Synechococcus* sp. (Msyn) and *Synechocystis* sp. (Syn) as well as C-termini of PspA of *Synechocystis* sp. and *Nostoc* (*Anabaena*) sp. were aligned with ClustalW 1.7 program. Identical amino acids are shown in black, similar amino acids are shown in grey. Motifs characteristics are depicted in red. An asterisk marks the position of the conservative LPP/LP. The scheme above the sequence represents the secondary structure prediction. The box designates the α-helical region. The random coil region is drawn as a line.

Apart from the presence of the LPP/LP motif, the amino acid sequence as well as the length of the Vipp1 C-terminal random coil is quite diverse in different organisms. The C-terminal α-helix, on the contrary, shows higher amino acid similarity and carries a conserved motif (I/V---EL--LR). The functional importance of the described structure remains unclear. One can speculate that the variable random coil region serves as a linker between the PspA-like part of Vipp1 and its C-terminal α-helical domain. The presence of prolins in the beginning of the random coil would allow it to bend against the rest of the protein making the C-terminal α-helix more flexible and thereby facilitating its interactions with the stromal or inner envelope partners.

6.2. Analysis of Vipp1 topology

6.2.1. Cross-linking experiments with inner envelope vesicles

Although Vipp1 is nominally a soluble protein, it was shown to be tightly associated with the inner envelope of pea (Li et al., 1994). This could be due to an interaction of

Vipp1 with membrane-embedded proteins in a fashion similar to PspA. To find out whether in chloroplasts the Vipp1 molecule is indeed in close proximity to other proteins, inner envelope membrane vesicles purified from pea chloroplasts were cross-linked with the membrane-impermeable cross-linker BS^3. After separating the proteins by SDS-PAGE they were analyzed by Coomassie staining and Western blotting with a Vipp1-specific antibody (Fig. 5).
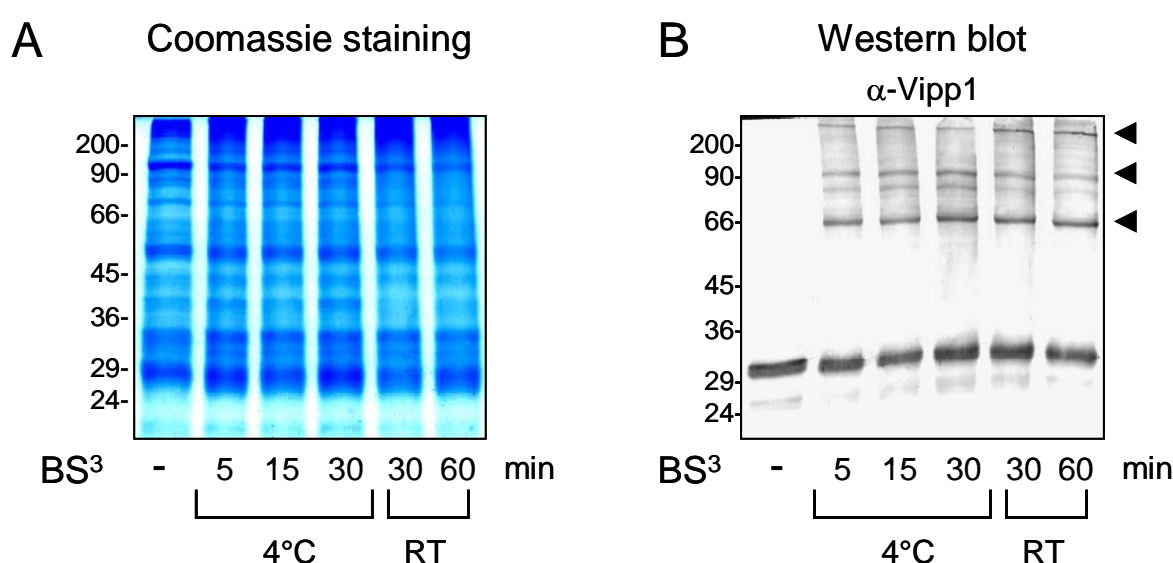

Figure 5: Cross-linking of inner envelope vesicles from pea with BS^3.

Proteins of purified inner envelope vesicles of pea were incubated with BS^3 for given periods of time, either at 4°C or at room temperature. The cross-linking reaction was analysed by SDS-PAGE and immunodecoration with an α-Vipp1-antibody. (A) Coomassie-stained gel. (B) Immunodecoration with α–Vipp1. Specific cross-link products are indicated by *arrows*.

The Coomassie-stained gel (Fig. 5 A) demonstrates that samples incubated with BS^3 for different periods of time do not show drastic changes in the protein pattern, indicating that no unspecific cross-linking event occurred. The immunodecoration with the α-Vipp1 specific antibody, on the other hand, showed that incubation with BS^3 results in the formation of several new immunoreactive bands (Fig. 5 B).

The monomeric Vipp1 can be detected as a band of 33 kDa, in accordance with its deduced molecular mass (Li et al., 1994; Kroll et al., 2001). A second band of about 35

kDa is frequently observed after long exposure to reducing conditions and was identified previously as Vipp1 by protein sequencing (Kroll et al., 2001). A band of approx. 66 kDa becomes visible early on during the cross-linking reaction (Fig. 5 B, min incubation at 4°C) and remains the most prominent cross-link product even after prolonged incubation with BS^3 (Fig. 5 B, 15 min and 30 min at 4°C, 30 min and 1 h at RT). The reaction also results in two other well pronounced immunoreactive bands, of about 100 kDa and over 200 kDa in size. The intensity of the 66 kDa and 100 kDa bands increases with time of incubation at 4°C (Fig. 5 B, compare 5, 15 and 30 min at 4°C). The largest cross-link product especially accumulates after long incubation at room temperature, indicating that under these conditions the reaction shifts toward formation of high-molecular weight products. The described pattern of cross-link products was observed repeatedly, supporting the specificity of the cross-linking reaction. These results indicate that Vipp1 is in close proximity to other proteins to which it can be cross-linked. The sizes of the cross-linking products are implicative of the formation of Vipp1 homodimer, -trimer and -octamer. This would suggest that Vipp1 primarily forms a homodimer or that it interacts with a protein of a very similar molecular mass.

6.2.2. BN-PAGE analysis of cyanobacterial and chloroplastidal Vipp1

The presence of new immunoreactive Vipp1 bands after cross-linking indicates that Vipp1 might be present in a protein complex. To investigate a possible complex formation by Vipp1, native protein complexes from chloroplasts of several higher plants or from total membranes of *Chlamydomonas reinhardtii* and *Synechocystis* sp. were analyzed by blue native polyacrylamid gel electrophoresis (BN-PAGE). Isolated *Arabidopsis* chloroplasts were solubilized with 1% n-Decyl-β-D-maltoside (DM) and non-solubilized proteins were removed by centrifugation. Under these conditions, most of the proteins were found in the supernatant including at least 95% of the Vipp1 protein as determined by Western Blot analysis (Fig. 6).

The solubilized proteins and protein complexes were subsequently separated on a 3%-13% gradient BN-PAGE in the first (Fig. 7 A, upper panel) and a 10% SDS-PAGE in the second dimension. Proteins were transferred onto a nitrocellulose membrane and immunodecorated with α−Vipp1 serum. Under these conditions Vipp1 could be identified in two distinct positions (Fig. 7 A, lower panel). A minor part of Vipp1 was found slightly below the first green band, which contains the monomeric light harvesting chlorophyll

binding proteins and corresponds to a size of about 66 kDa. This part of the Vipp1 protein is therefore most likely monomeric. The major part of Vipp1 was found clearly above the PSI super-complex corresponding to a size of well over 1000 kDa, indicating that most of the Vipp1 is present in a high molecular weight complex. Similar results were obtained from BN-PAGE analyses of isolated chloroplasts of *Pisum sativum* and *Nicotiana tobacco* (data not shown) providing evidence that this feature of Vipp1 is common to chloroplasts of all higher plants.
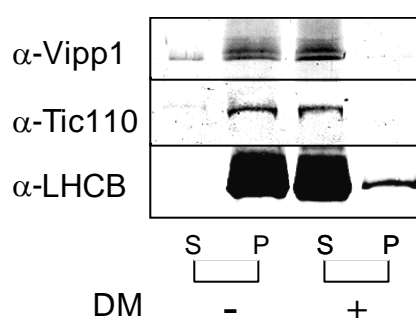
Figure 6: Solubilisation of Vipp1 with n-Decyl-β-D-maltoside.
Arabidopsis chloroplast lysates without (-) or after (+) treatment with DM were separated into soluble fraction (S) and pellet (P) by centrifugation at 21000xg for 10 min. The samples were applied to SDS-PAGE, transferred onto nitrocellulose membrane and immunodecorated with α-Vipp1, α-Tic110 and α-LHCB antibodies.

To elucidate whether such a Vipp1 complex is also found in algae, BN-PAGE analysis was performed on total membranes of *Chlamydomonas reinhardtii*. Total membranes were isolated and as before solubilized with DM. Solubilized proteins were subjected to BN-PAGE (Fig 7B, upper panel) and subsequently to SDS-PAGE. After Western blotting, Vipp1 was visualized by the α-Vipp1 made against the pea protein. As with higher plants, part of Vipp1 could be identified in a position indicative of a high molecular weight complex (Fig. 7 B, lower panel). In comparison with *Arabidopsis*, more of Vipp1 was found in the monomeric form. This can either reflect a slightly different *in vivo* situation in *Chlamydomonas* cells or could be caused by a higher susceptibility of *Chlamydomonas* protein complexes to disintegrate upon solubilisation with DM.
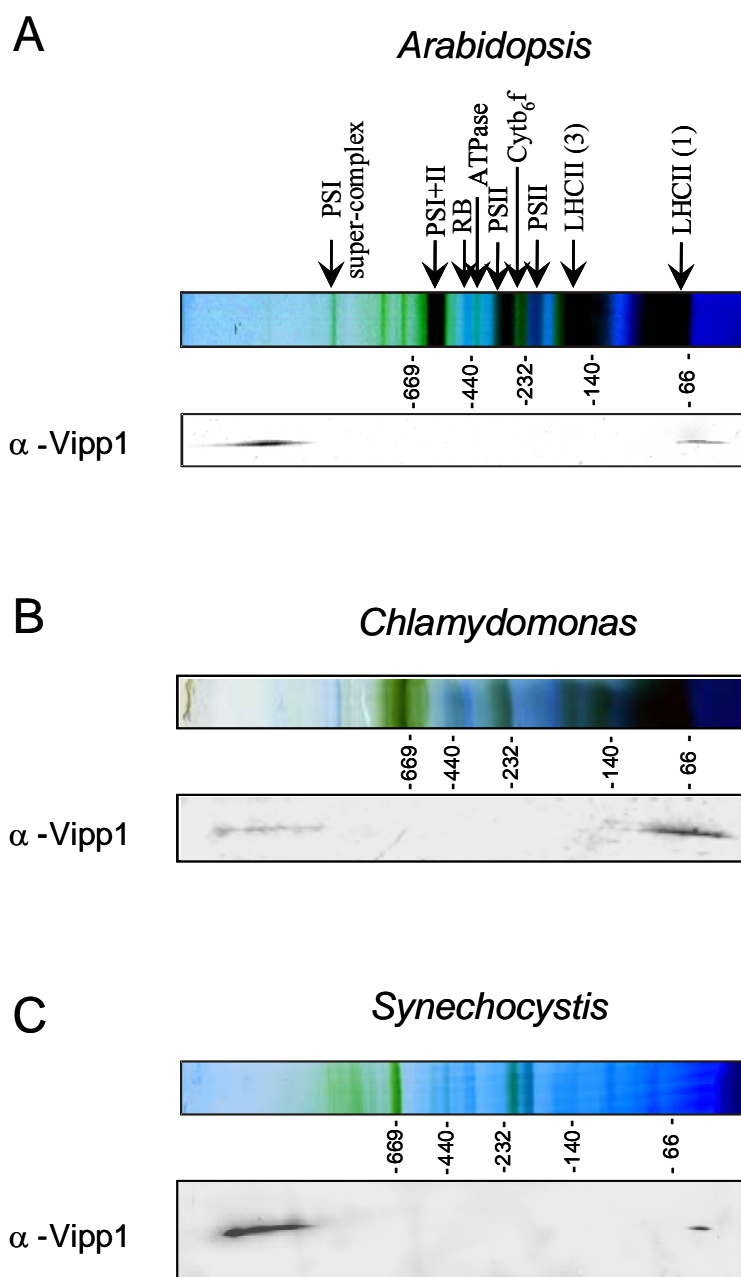
Figure 7: Vipp1 is assembled in a high-molecular-weight complex of over 1000 kDa size.

Freshly isolated *Arabidopsis thaliana* chloroplasts (A) or total membranes of *Chlamydomonas reinhardtii* (B) and *Synechocystis* sp. 6803 (C) were solubilized with 1% DM and separated on 3%-13% BN-PAGE in the first (*upper panels of A, B and C*) and 10% SDS-PAGE in the second dimension. Positions of main photosynthetic complexes are shown for *Arabidopsis* (*upper panel*). Immunodecoration shows Vipp1 in two distinct positions corresponding to the likely monomeric protein and a complex of well over 1000 kDa (*lower panels*).

The data obtained for higher plants and algae indicate that the presence of Vipp1 in a complex is common for chloroplasts. Since cyanobacteria are the ancestor of these organelles and also require Vipp1 for their thylakoid biogenesis (Westphal et al., 2001a), it was studied whether a similar organization of Vipp1 can be found in *Synechocystis* cells. Total membranes of *Synechocystis* sp. PCC 6803 were isolated and solubilized with DM. BN-analysis was performed as described for *Arabidopsis* and *Chlamydomonas*. Western Blot with α-Vipp1 showed very little Vipp1 in the monomeric form, while most of the Vipp1 was present in a position of similar size compared to higher plants and *Chamydomonas* (Fig. 7 C). Thus, like in higher plants and algae, Vipp1 of *Synechocystis* is part of a high molecular weight complex.

6.2.3. Trypsin digestion of inner envelope vesicles of *Pisum sativum*

Hydropathy analysis of Vipp1 does not reveal any membrane-spanning domains. Nevertheless, Vipp1 is found tightly associated with both the inner envelope and thylakoids of pea (Keegstra et al., 1994) and *Arabidopsis* (Kroll et al., 2000), and with the plasma membrane of *Synechocystis* (Westphal et al., 2001a). To closer elucidate the nature of this membrane association and the topology of Vipp1, inner envelope vesicles of pea were treated with trypsin. The incubation with an increasing concentration of trypsin results in the formation of a 25 kDa proteolytical fragment of Vipp1 that remained highly resistant to further proteolysis (Fig. 8, first panel). Taking in consideration the homology of Vipp1 and PspA and the fact that part of PspA protein is found to be peripherally bound to the bacterial inner membrane (Kleerebezem and Tommassen, 1993), a comparable trypsin digestion of *E. coli* lysates was performed with the trypsin concentrations as for pea inner envelope vesicles (Fig. 8, third panel). Partial degradation of PspA was observed under these conditions, which can be seen by comparing band intensities in immunoblotting before and after trypsin treatment. However, some part of PspA remained protected from degradation and other than with Vipp1 no additional proteolytical subfragments was detected (Fig. 8, third panel). The fact that part of PspA remains stable and part proteolitically degrades is in agreement with the observation that in a bacterial cell PspA is found in an inner membrane fraction as well as in a soluble pool. On the other hand, it
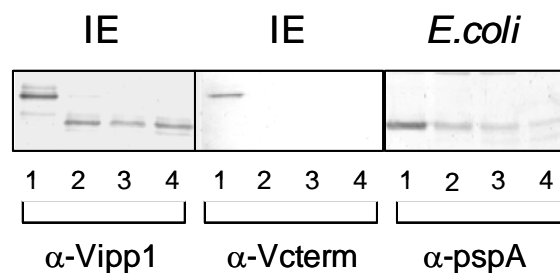
Figure 8: Trypsin digest and BN- PAGE analysis of Vipp1.

Inner envelope vesicles of pea chloroplasts were treated with increasing concentrations of trypsin: 1 - no trypsin; 2 – 3.3 µg/ml; 3 – 10 µg/ml; 4 – 20 µg/ml. The samples were separated by SDS-PAGE and analysed in Western blotting with anti-Vipp1 antibody that recognize the full length protein (α-Vipp1) and with antibody specific for the C-terminal domain of Vipp1 (α-Vcterm). Trypsin treatment resulted in the formation of a proteolitically resistant 25 kDa Vipp1 fragment which was not recognized by α-Vcterm antibody. As a control, *E. coli* membranes were treated with trypsin as indicated above and immunodecorated with α-pspA.

cannot be excluded that under chosen conditions the bacterial membrane is in general more sensitive to trypsin treatment resulting in the enhanced susceptibility of PspA in comparison to Vipp1.

The 25 kDa fragment obtained after proteolysis of Vipp1 very much resembles in size PspA from *E. coli*. Moreover, secondary structure prediction of Vipp1 indicates that its N-terminal PspA-like domain possess an α-helical structure, which is separated from the C-terminal α-helix by a random coil spacer, a new acquisition of all Vipp1 proteins. Therefore, it seemed possible that the protease can access Vipp1 at this unstructured region, cleaving off the C-terminal extension, while the PspA-like domain remains protected. Indeed, a potential trypsin cleavage site is located just at the beginning of the random coil spacer. To test this assumption an antibody against the last 42 amino acids of the pea Vipp1 protein (α -Vcterm) was raised. The antiserum recognized the full length Vipp1 protein in untreated inner envelope. In contrast, the 25 kDa peptide that remained after trypsin digestion was not recognized by this antibody (Fig. 8 A, second panel). This result confirms that it is the PspA-like region of Vipp1 which is resistant to proteolysis. In
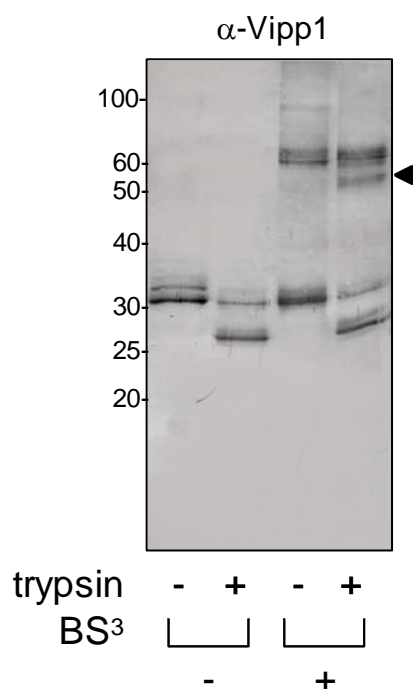
α-Vipp1

trypsin   -   +   -   +

BS³

Figure 9: Trypsin digest of pea inner envelope followed by BS³ cross-linking.
Pea inner envelope vesicles were treated with 15 µg/ml of trypsin for 90 sec. After the reaction was stopped, the sample was divided in two and incubated for 1 h with or without BS³. As control, BS3 cross-linking without trypsin treatment was performed. The proteins were analysed by Western blotting with α-Vipp1 antiserum. The arrow indicates a Vipp1 immunoreactive band of approx. 50 kDa specifically appearing in BS3 cross-linking of trypsin-treated sample.

contrast, the Vipp1-specific carboxyterminal extension is accessible for other proteins and is cleaved from the Vipp1 protein upon trypsin treatment. The cross-link of inner envelope vesicles with BS³ indicates that Vipp1 can either build homodimers and –multimers or interact with a protein of similar size. The domain required for this interaction could be localized either in the N-terminal PspA-like region of Vipp1 or its C-terminal part. Therefore it was elucidated whether the N-terminal domain of Vipp1 derived from proteolysis is sufficient to promote dimer formation. To study this question, inner envelope vesicles were first treated with trypsin and then cross-linked with BS³. Beside the formation of the 25 kDa proteolitical fragment, two bands were observed in immunoblotting with α-Vipp1 (Fig. 9). The band of 66 kDa is identical in size to the band obtained when the cross-link alone is performed. This band is most probably created by a non-digested full-size Vipp1. The second band of about 50 kDa was observed exclusively when the inner envelope was treated with trypsin prior to cross-link (Fig. 9, indicated by arrow). The size of this band corresponds to twice the Vipp1 25 kDa proteolytical fragment. The presence of the 50 kDa band indicates that the proteolitically resistant N-terminal region of Vipp1 is sufficient to form a cross-link product. Moreover, the size of this product, which is twice the size of the proteolitically resistant region of Vipp1, indirectly supports the supposition about Vipp1 homodimer formation.

Since Vipp1 is not a transmembrane protein, the proteolitical resistance of its N-terminal part can not be explained by its insertion into a membrane bilayer. Vipp1 could rather be protected from proteolysis by tight association with a membrane or by complex formation. To elucidate the nature of the Vipp1 proteolitical resistance, inner envelope proteins were first released from the membrane by treatment with 1% DM and then
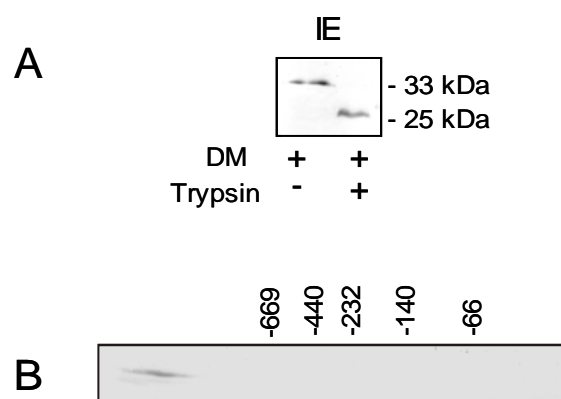

Figure 10: Analysis of Vipp1 proteolysis in the presence of detergent.

(A) Inner envelope was solubilized with 1% DM before trypsin treatment. Proteins were separated by SDS-PAGE and immunodecorated with α-Vipp1. (B) Inner envelope proteins treated as in A were subjected to BN-PAGE prior to SDS-PAGE and subsequently analysed in immunoblotting with α-Vipp1 antiserum.

incubated with trypsin (Fig. 10). If the interaction with the membrane is the cause of Vipp1 trypsin resistance, the 25 kDa proteolytical fragment will not be detected under these conditions, as Vipp1 will be devoid of the lipid environment. On the other hand, if the insensitivity to proteolysis is due to tight complex formation, i.e., in the manner described for α-helical SNARE proteins, the 25 kDa fragment will be formed even in the presence of detergents. Immunodecoration with α-Vipp1 revealed a 25 kDa band in the sample treated with trypsin after DM-solubilization, indicating that complex formation is a likely reason for Vipp1 proteolytical resistance (Fig. 10 A). To further support this idea, the proteins were separated on BN-PAGE prior to SDS-PAGE and again immunodecorated with α-Vipp1. No reaction was detected at the low molecular weight size as it would be expected for a 25 kDa fragment in a monomeric form. Instead, the Vipp1 proteolytical fragment was exclusively found at the position of over 1000 kDa, which indicates its assembled state

(Fig. 10 B). These results imply that the N-terminal PspA-like domain of Vipp1 remains proteolytically resistant due to its assembly in a complex. The Vipp1-specific C-terminal extension is not buried within the complex and therefore accessible to proteolysis.

6.2.4. BN-PAGE analysis of heterologously expressed Vipp1

The data obtained from the cross-linking studies indicate that a Vipp1 complex might be formed by multiple subunits of Vipp1. Moreover, the arrangement in a large homooligomeric complex has been shown for PspA of *E. coli* (Hankamer et al., 2004). To elucidate whether the formation of Vipp1 complex occurs in a similar manner or requires specific plant components, *E. coli* cells overexpressing Vipp1 from *Arabidopsis* were analysed for the presence of a Vipp1 complex.

The full length Vipp1 from *Arabidopsis* with an N-terminally fused 6xHis-tag was heterologously expressed in *E. coli.* The cells were disrupted and the soluble and membrane fractions were analysed by SDS-PAGE. The majority of the heterologously expressed 6xHis-Vipp1 was detected in the fraction containing insoluble proteins and only a minor part was found soluble (Fig. 11 A). The membrane fraction was subsequently treated with DM, and solubilized proteins were separated by BN-PAGE and SDS-PAGE as before. Western Blot analysis revealed that more than half of the Vipp1 protein
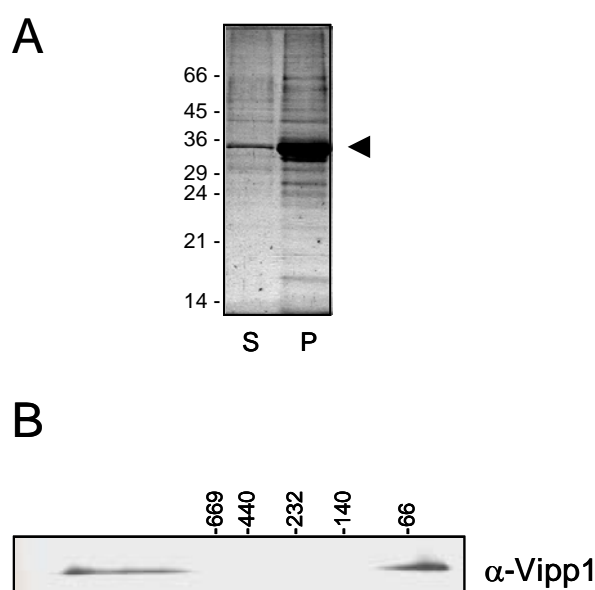

Figure 11: Heterologously expressed Vipp1 forms a high molecular weight complex.

(A) *E. coli* cells overexpressing 6xHis-Vipp1 were disrupted by passage through a French pressure cell. The sample was divided into soluble (S) and insoluble (P) fractions by centrifugation and analyzed on SDS-PAGE. Most of Vipp1 is found in the membrane fraction (indicated by arrow). (B) After solubilization with 1% DM, the membrane fraction was further analyzed by BN-PAGE followed by SDS-PAGE in the second dimension. Western blotting with α-Vipp1 antiserum revealed a reaction at the positon of Vipp1 monomer as well as Vipp1 high molecular weight complex.

was present as monomeric protein. Nevertheless, a significant amount was found in a high molecular weight complex of approximately the same size as native Vipp1 from chloroplasts (Fig. 11 B). These results indicated that heterologously expressed Vipp1 protein alone seems to be sufficient for complex formation and no particular chloroplast proteins are required for this process.

6.2.5. Analysis of heterologously expressed Vipp1 by size exclusion chromatography

To obtain more information about the nature of the Vipp1 complex, heterologously expressed Vipp1 protein was purified from *E. coli* cells and analyzed by size exclusion chromatography. Two different approaches of purification were applied and compared. Firstly, Vipp1 complex was purified under non-denaturing conditions. A minor part of heterologously expressed Vipp1 is soluble under conditions where the non-denaturing detergent CHAPS is used in the preparation (data not shown). Therefore, *E. coli* cells expressing 6xHis-Vipp1 were disrupted, the Vipp1-containing membrane fraction was incubated with 1.1% CHAPS and the solubilized proteins were collected after centrifugation. Solubilized Vipp1 was purified by affinity chromatography on Ni-NTA under non-denaturing conditions and the eluate was further separated by size exclusion chromatography on Superose 6 HR 10/300 (Fig. 12 A). The chromatogram displayed a major protein peak corresponding to a molecular mass of about 2000 kDa. Western Blot analysis identified Vipp1 in this high-molecular weight peak (Fig. 12 A) confirming the results from the BN-PAGE analysis.

The behavior of the heterologously expressed Vipp1 protein during size exclusion is identical to that of Vipp1 purified from detergent-solubilized chloroplasts, providing confirmation that the heterologously expressed Vipp1 behaves like the native protein (data not shown). However, the above approach could not provide sufficient amount of protein for a further detailed analysis of the Vipp1-complex. Therefore, a larger quantity of purified Vipp1 was obtained from a non-soluble *E. coli* fraction by renaturing of urea-solubilized protein. Vipp1 was first purified on Ni-NTA matrix under denaturing conditions and subsequently incubated in a buffer which included PEG, sucrose and 550 mM guanidine-HCl. This buffer was chosen from the Foldlt Screen protocol for protein renaturation since under these conditions a significant part of Vipp1 appeared to be soluble (data not shown). Precipitated Vipp1 was discarded after centrifugation and the
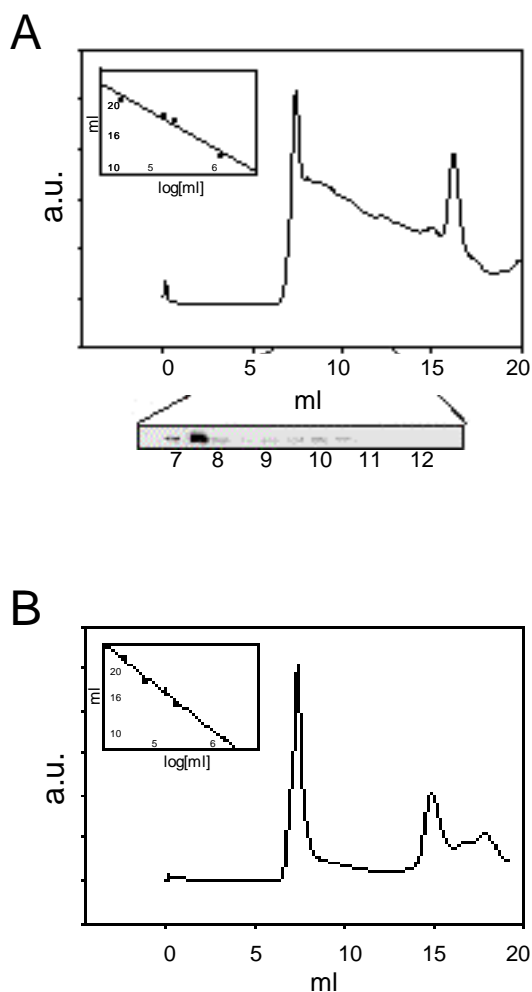
A

Figure 12: Chromatography of heterologously expressed Vipp1 protein by size exclusion.

(A) Heterologously expressed Vipp1 was purified by nickel affinity chromatography under native conditions and analyzed on Superose 6 HR 10/300 column. The inset depicts the column calibration. The chromatogram displays the major elution peak at 7.5 ml corresponding to a molecular weight of approximately 2000 kDa. Western blot analysis with α-Vipp1 antiserum confirmed that the majority of Vipp1 elutes in this peak. Protein from the peak fraction was later used for analysis by EM negative staining (see Fig. 13 a). (B) Heterologously expressed Vipp1 purified under denaturing conditions and subsequently renatured was analyzed on Superose 6. The inset depicts the column calibration. The majority of Vipp1 protein eluted as a high molecular mass complex corresponding to a size of approximately 2000 kDa. Protein from the peak fraction was later used for negative staining EM analysis (see Fig. 13 b).

B

supernatant was dialysed. This fraction was then likewise analysed by size exclusion chromatography (Fig. 12 B). The chromatogram obtained from this fraction was very similar to the one from Vipp1 purified under non-denaturing conditions. The Vipp1 protein was again predominantly in the peak corresponding to a molecular weight of approximately 2000 kDa. Thus, the performed cycle of denaturation – renaturation did not interfere with the ability of Vipp1 to form a high molecular weight complex.

The eluates of the high-molecular peak fractions obtained in both Vipp1 purification approaches were further used for electron microscopic studies.

6.2.6. Analysis of purified Vipp1 complex by negative staining electron microscopy

The purified complex was visualized by negative stain electron microscopy. The initial analysis was performed on the Vipp1 complex purified by size exclusion chromatography

under non-denaturing conditions, as this purification procedure more likely provides the Vipp1 complex in its native state. Due to the limited amount of protein the sample yielded only very few particles (Fig. 13, panel a). More data on the Vipp1 particles were obtained by the analysis of Vipp1 complexes isolated under denaturing conditions, subsequently renatured and further purified by size exclusion (Fig. 13, panel b and c). These samples yielded a much larger set of particles. Electon micrographs obtained from both purification techniques were compared in order to get an impression of the shape of the Vipp1 complex. Both purification approaches provided a set of particles of similar size and appearance, therefore the images of Vipp1 complex purified by denaturation / renaturation technique were considered as representative and analyzed in detail.
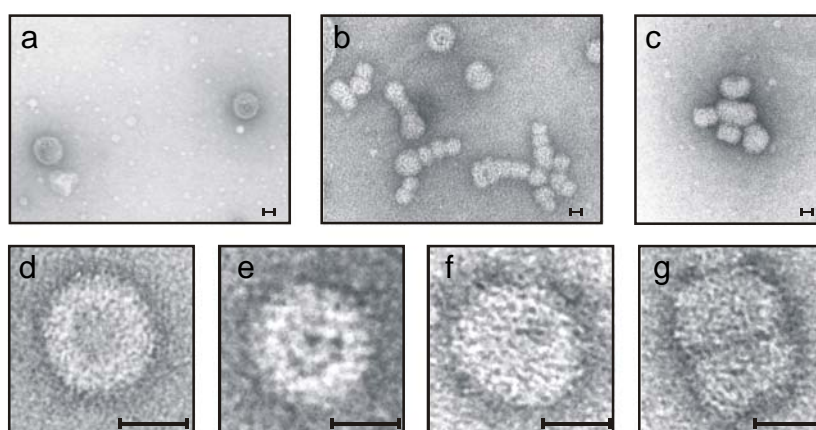
Figure 13: Analysis of Vipp1 complex by negative stain electron microscopy.
Pictures were obtained from samples purified either under native conditions (*a*) or under denaturing conditions followed by renaturation (*b–g*). Overview pictures show the presence of single complexes as well as aggregated complexes in the different preparations (*a–c*). Enlargements of single complexes were used to estimate the dimension of the complexes (d–g). d, e – Top view on Vipp1 complex; f – tilted particle; g – side view on two Vipp1 complexes in a stack. The bar corresponds to 100 Å.

The majority of singular particles appeared ring-shaped, with a darker area in the center (Fig. 13, panel a, b, d, and e) and they were classified as top view onto the complex. Other particles appeared tilted in reference to the plane of the grid, representing a side view on the complex (Fig.13, panel b, g). These particles were often found in stacks of two or more. It was observed that this stacking increases in the samples with a higher complex

concentration. In some rare cases particles could be found which were tilted at less than 90 degree angle (Fig.13, panel c and f). In these cases the hole in the middle of the complex became partially visible. To get a rough estimation of the size of the Vipp1 complex, the dimensions of about 60 single particles were measured. Calculated from these measurements the Vipp1 complex has a width of about 400 Å and a height of about 140 Å. The hole in the middle is estimated to be about 120 Å.

6.2.7. Transient expression of Vipp1 in protoplasts

The fact that most of Vipp1 is organized in a high molecular weight complex raised the question of where this large complex is localized within the organelle. The localization of Vipp1 in chloroplasts was visualized by GFP-fusion technique. The *VIPP1* gene of *Arabidopsis* including its presequence was N-terminally fused to the green fluorescence protein (GFP) sequence in the pOL-GFP vector. The 35S CaMV promoter allowed transient expression of the resulting construct (pVipp1-GFP) in tobacco protoplasts. As shown in figure 14 (panel b), the Vipp1-GFP fusion protein is targeted into the chloroplasts
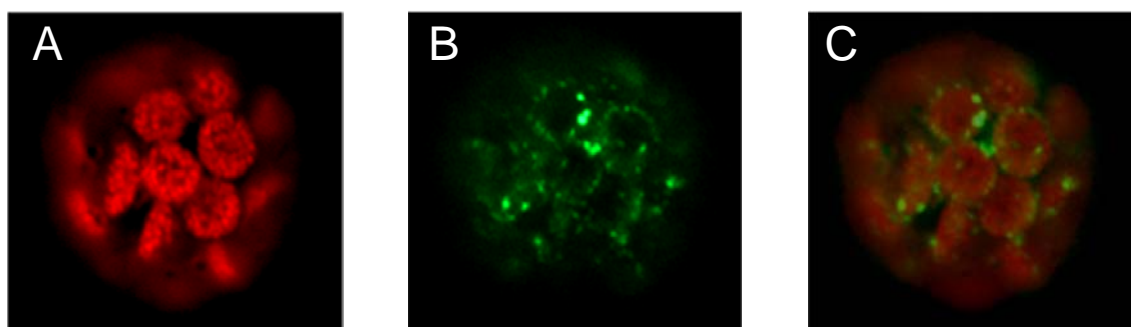

Figure 14: Localization of pVipp1-GFP in tobacco protoplasts.
Isolated tobacco protoplasts were transformed with pVipp1-GFP and expressed Vipp1-GFP fusion was visualized by fluorescent microscopy. (A) Chlorophyll fluorescence. (B) Vipp1-GFP fluorescence. (C) Overlay of A and B.

where it is found in many well defined spots arranged in a ring-like fashion. An overlay of the chlorophyll (Fig. 14 B, panel a) and the GFP fluorescence signals indicated that Vipp1-

GFP resides outside the thylakoid membrane system (Fig. 14 B, panel c). This pattern is consistent with a location of the Vipp1-GFP fusion protein either inside the inner envelope or close to the inner surface of the chloroplasts envelope.

To study the Vipp1 localization in more details, two further GFP-fusion constructs were made: pVipp1m-GFP, which comprises only the PspA-like domain of Vipp1 without its
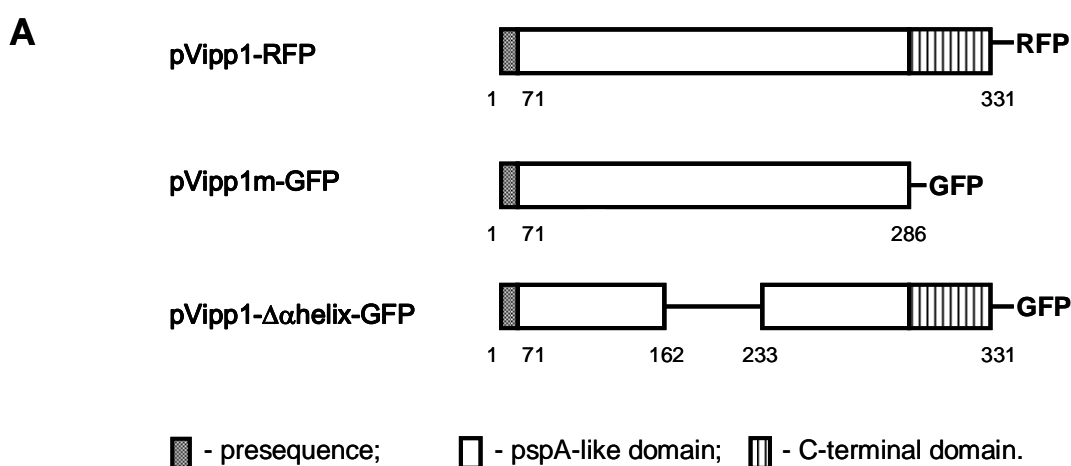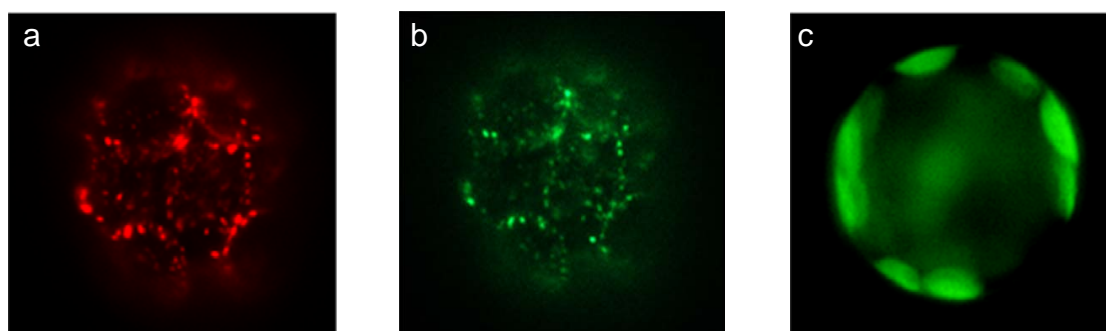

Figure 15: Fluorescence micrographs of protoplasts transformed with different Vipp1-GFP/RFP fusions.

(A) Schematic representation of the constructs used for protoplast transformation. (B) Localization of the Vipp1-fusions depicted in A. a, b, - a protoplast expressing both Vipp1-RFP (a) and Vipp1m-GFP (b); c - transient expression of Vipp1-Δα- helix-GFP.

C-terminal extension, and pVipp1Δα-helix-GFP, where 54 amino acid residues of the long α-helical stretch inside the PspA-like domain of the protein were removed (Fig. 15 A). To distinguish the localization of these constructs from the full length Vipp1, pVipp1 was subcloned into pOL-RFP vector thereby creating pVipp1-RFP. The latter was used for co-transformation with pVipp1m-GFP and pVipp1Δα-helix-GFP in protoplasts of tobacco (Fig. 15 B) and *Arabidopsis* (data not shown).

The Vipp1m-GFP protein displayed the same distribution pattern as Vipp1-GFP. Indeed, double transformations with both constructs into the same protoplast revealed the proteins in indistinguishable spots indicating that they are present in identical complexes (Fig. 15 B). An overlay of the chlorophyll (Fig. 14 B, panel a) and the GFP fluorescence signals indicated that Vipp1-GFP resides outside the thylakoid membrane system (Fig. 14 B, panel c). This pattern is consistent with a location of the Vipp1-GFP fusion protein either inside the inner envelope or close to the inner surface of the chloroplasts envelope. On the other hand, no ring-like pattern was observed with Vipp1Δα-helix-GFP (Fig. 15 B, panel f). Instead, the fluorescence signal was distributed evenly throughout the chloroplasts as would be expected from a soluble stroma protein. Thus, disruption of the central α-helical part of the Vipp1 proteins inhibits the localization of Vipp1 to the inner envelope. Taken together, the GFP-fusion approach showed that the central α-helical region of Vipp1 and not its C-terminal domain is responsible for the proper localization of Vipp1 in chloroplasts.

6.2.8. BN-PAGE analysis of protoplasts transformed with GFP fusion proteins

To test whether full length Vipp1 fused to GFP supports complex assembly and therefore reflects the behavior of endogenous Vipp1, a combination of GFP-transformation and BN-PAGE technique was used. The analysis of various GFP-fusion constructs on BN-PAGE also allowed obtaining more information about the involvement of different regions of Vipp1 in the complex formation.

Chloroplasts from protoplasts transformed with different GFP-fusion constructs were isolated, separated by BN- and subsequently by SDS-PAGE and analyzed by Western Blot with α-Vipp1 antiserum. Both the endogenous Vipp1 (33 kDa; Fig. 16, second panel) and the Vipp1-GFP fusion protein (45 kDa; Fig. 16, third panel) were visible on the blot due their difference in molecular weight. They both displayed a similar distribution between the low-molecular weight and the complex form thereby validating the functionality of

Vipp1-GFP. Western blot analysis of protoplasts transformed with Vipp1m-GFP construct gave a similar result (Fig. 16, fourth panel). In contrast, the Vipp1Δα-helix-GFP protein was found exclusively as a monomeric protein (Fig. 16, fifth panel) indicating that complex formation is abolished. Thus, the combination of fluorescence microscopy and BN-PAGE analysis shows that a domain (or domains) responsible for complex formation and its localization on the inner envelope of chloroplasts lays within the central α-helical region of Vipp1, while the Vipp1-specific C-terminus has no influence on either.
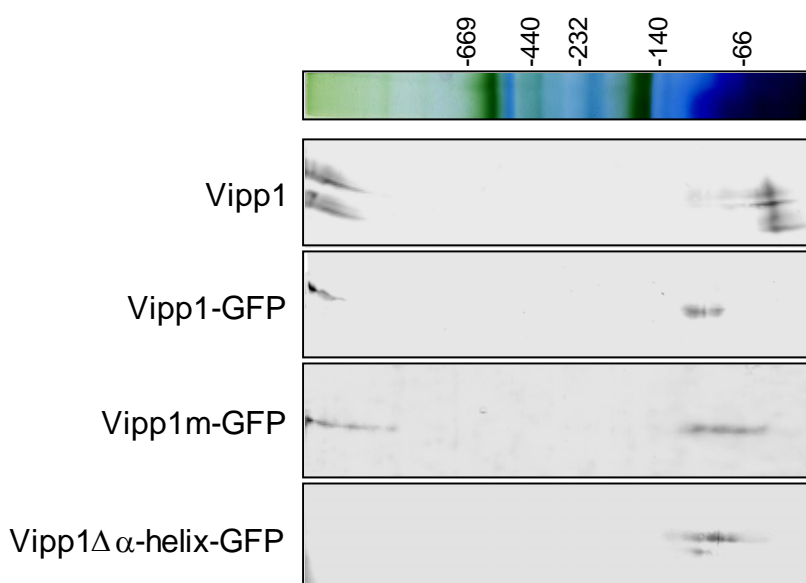
Figure 16: BN-PAGE analysis of Vipp1-GFP fusion protein expressed in protoplasts.
Analysis of tobacco protoplasts transiently transformed with different GFP fusion constructs is shown. Chloroplast proteins were isolated, separated by BN-PAGE (*top panel*) in the first and by SDS-PAGE in the second dimension and probed with α-Vipp1 antiserum. The antibody recognizes the endogenous Vipp1 (*second panel*), the transiently expressed Vipp1-GFP (*third panel*), Vipp1m-GFP (*fourth panel*) and Vipp1Δα-helix-GFP (*fifth panel*).

6.3. Analysis of Vipp1-ProtA plants

Analysis of mutants is a powerful tool to approach the function of a specific gene. Disruption of the *VIPP1* gene locus in *Arabidopsis* results in a nearly complete loss of

thylakoids in the chloroplasts of the mutant plants, indicating important role of Vipp1 in the process of thylakoid formation (Kroll et al., 2001). Consequently, the photosynthetic capacity of such plants is greatly reduced; they are only capable of heterotrophic growth and develop an albinotic phenotype (Kroll et al., 2001). As a result, Δ*vipp1* displays a number of secondary effects that cannot be directly correlated to the function of the mutated gene. In contrast, plants displaying a less drastic reduction in Vipp1, could provide a tool to elucidate the primary effects of Vipp1 deficiency thereby allowing to come closer to understanding of the Vipp1 function.

6.3.1. Characterisation of Vipp1-ProtA plants

Vipp1-ProtA plants were made by introducing a cDNA coding for the *Arabidopsis VIPP1* gene (At1g65260) C-terminally fused to the IgG-binding domain of the *PROTEINA* gene from *Staphylococcus aureus* into Δ*vipp1* plants by *Agrobacterium tumefaciens* mediated transformation (Stein, 2004). The fusion construct (*VIPP1-PROTA*) is expressed under the CAMV-35S promoter. The plants were made by Bernhard Stein in the laboratory of Prof. Westhoff and were given to our laboratory for further characterisation.

Transformants were initially selected for plants homozygous for the Δ*vipp1* mutation but heterozygous with respect to the *VIPP1-PROTA* insertion. Seeds from these plants segregated according to the *VIPP1-PROTA* insertion. Approximately 25% of the plants were homozygously not carrying the insertion and these plants resembled the true Δ*vipp1* mutant phenotype. In contrast, about 75% of the transformants were able to grow photoautotrophically on soil. These plants are either heterozygous or homozygous for the *VIPP1-PROTA* insertion and they did not display a distinctive phenotype when grown under low light conditions (< 20 μmol photons m^{-2}s^{-1}), indicating that the fusion protein is able to substitute for Vipp1 function. Surprisingly, when grown under high light conditions (> 70 μmol photons m^{-2}s^{-1}), only a smaller fraction still resembled wild type plants (Fig. 17 A, No. 11). The majority of plants were reduced in growth and the leaves showed different shades of pale-green (Fig. 17 A, No. 5). When analysed by Western blot with a Vipp1-specific antibody (Fig. 17 B, No. 11, 5 and 4), the α-Vipp1 antiserum detected a protein of 42 kDa, which corresponds to the expected size for the fusion protein of Vipp1 and the IgG domain of ProteinA, showing that *VIPP1-PROTA* construct is indeed expressed in these plants. From their appearance, the No. 11 plant resembled wild type, while both No. 4 and 5 displayed the pale-green phenotype. Since both types of plants

carry the *VIPP1-PROTA* insertion (data not shown), the observed alteration in phenotype
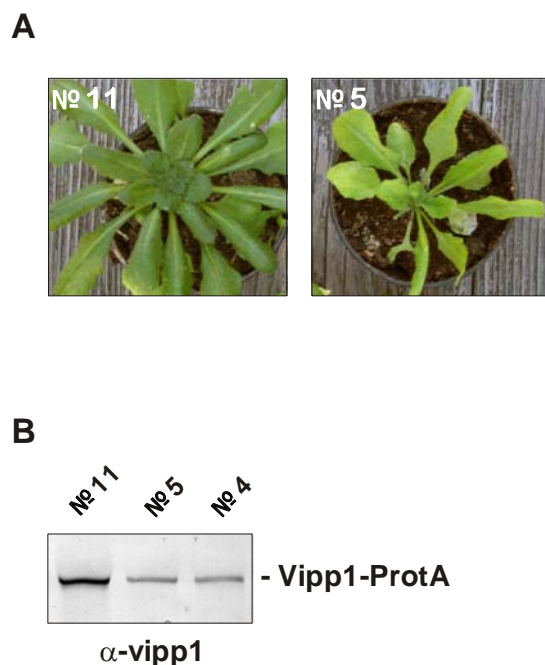
A

Figure 17: Phenotypic variation between plants carrying the *VIPP1-PROTA* insertion.
(A) Two representative Vipp1-ProtA plants grown on soil for 5 weeks.
(B) Immunodecoration of total leaf extracts from three Vipp1-ProtA plants with an α-Vipp1 antiserum.

B

appears to represent the difference between plants being either homozygous or heterozygous for the insertion, which is in accordance with the observed number of plants of each type in a mendelian segregation.

It thus appears that when present in a single copy, the *VIPP1-PROTA* insertion is not sufficient to fully restore the wild type phenotype of these plants. Instead, their phenotypes seem to represent an intermediate state between the original Δ*vipp1* mutant and wild type. This becomes even more evident if to compare heterozygous *VIPP1-PROTA* plants (further on referred to as K2) to Δ*vipp1* and wild type plants, all of which were grown heterotrophically on agar in normal light (Fig. 18 A). Early in plant development, leaves of the Δ*vipp1* mutant are still light green but in older plants their colour changes to completely white. In contrast, K2 plants are significantly larger then Δ*vipp1* and they do not bleach but also do not reach the size of wild type plants and remain paler in colour. When analysed by PCR, the K2 plants were indeed shown to be homozygous for the Δ*vipp1* T-DNA and to carry the *VIPP1-PROTA* insertion (Fig. 18 B).
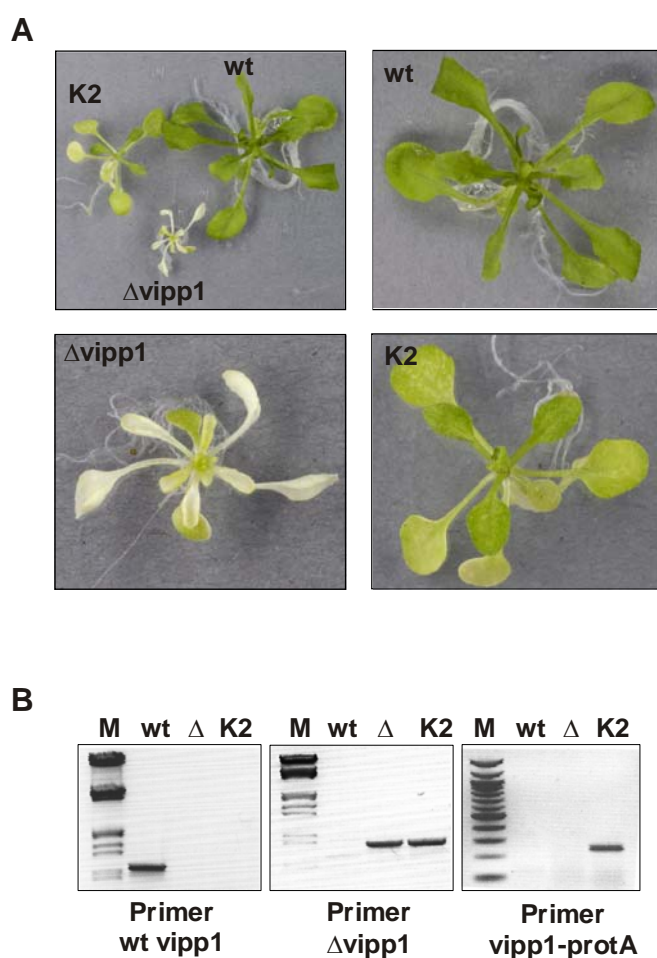
Figure 18: Complementation of the Δ*vipp1* (hcf155) mutant with *VIPP1-PROTA*.
(A) Seedlings of wild type (wt), K2 and Δ*vipp1* plants heterotrophically grown for 3 weeks. The upper left panel shows a comparison of typical plants to illustrate the difference in size and pigmentation. Other panels show respective enlargements. (B) PCR analysis of wild type (wt), Δ*vipp1* (Δ) and K2 plants with primers specific for the *vipp1* gene (left panel), the T-DNA insertion disrupting the *vipp1* gene (middle panel) and for the *VIPP1-PROTA* insertion (right panel).

6.3.2. Spectroscopic analysis of the photosynthetic electron-transport chain in Δ*vipp1* and K2 plants

To test whether the outward phenotype of the K2 plants is corroborated by their photosynthetic capacity, the activity of the photosynthetic electron transfer machinery of K2 plants was elucidated in comparison to both wild type and Δ*vipp1* mutant.

6.3.2.1. Measurement of chlorophyll fluorescence emission at 77K

In a first step, measurement of chlorophyll fluorescence was performed on isolated chloroplasts of wild type, K2 and Δ*vipp1*. Extracts of K2 and wild type plants were adjusted to equal amounts of chlorophyll. Samples from the Δ*vipp1* mutant were not

adjusted since their chlorophyll content is already very low. Measurement of chlorophyll fluorescence emission at 77K shows that the characteristic emission band for PSI at 35 nm
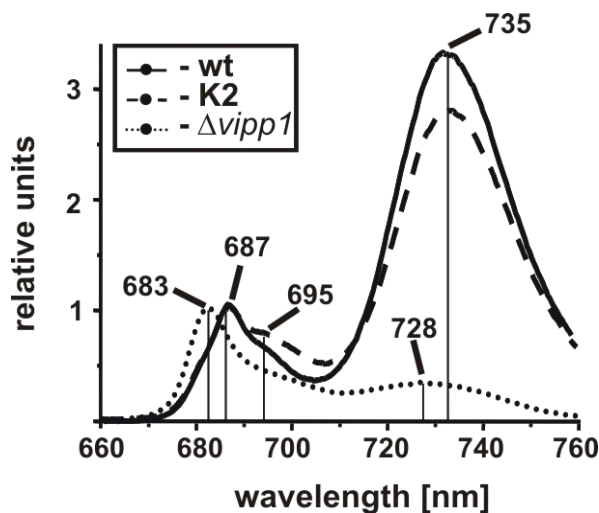

Figure 19: Analysis of 77 K chlorophyll fluorescence emission of wild type (wt), K2 and Δ*vipp1* plants.
Leaf tissue was ground in isolation buffer, filtered and frozen in liquid nitrogen. Equal amount of wt, K2 and Δ*vipp1* leaf tissue (fresh weight) was taken for each sample. Measurements were performed with excitation light of $\lambda = 430$ nm.

is highly reduced and a distinct shift to 728 nm can be observed (Fig. 19, dotted line). Furthermore, the characteristic PSII fluorescence peaks at 687 nm and 695 nm (CP43 and CP47, respectively) are not detectable, probably due to the enhanced emission at 683 nm overlapping with the residual PSII fluorescence. This shift in the emission peaks can be explained by a disruption of energy transfer from the antennae to the photosystems and could indicate that the light harvesting complex (LHC) antennae are no longer properly attached to the PSII core complex. In contrast, the chlorophyll emission spectra of K2 plants is very much similar to the wild type (Fig. 19, dashed line compared to solid line), which is in accordance with the restoration of autotrophic growth.

6.3.2.2. Analysis of photosynthetic activity of K2 and Δ*vipp1*

Photosynthetic activity was determined by measuring non-invasive chlorophyll fluorescence of dark-adapted plants under different intensities of actinic light ranging from 3.5 to 76.0 μmol photons $m^{-2}s^{-1}$ (Fig. 20). The first saturating pulse (800 ms) determined the maximal chlorophyll fluorescence (F_m) after dark incubation. After the application of actinic light, repetitive saturating flashes were given in intervals of 20 s and the efficiency of the light reactions during induction (F_m') was recorded. In K2 plants the level of minimal fluorescence appeared to be intermediate between the low level characteristic for
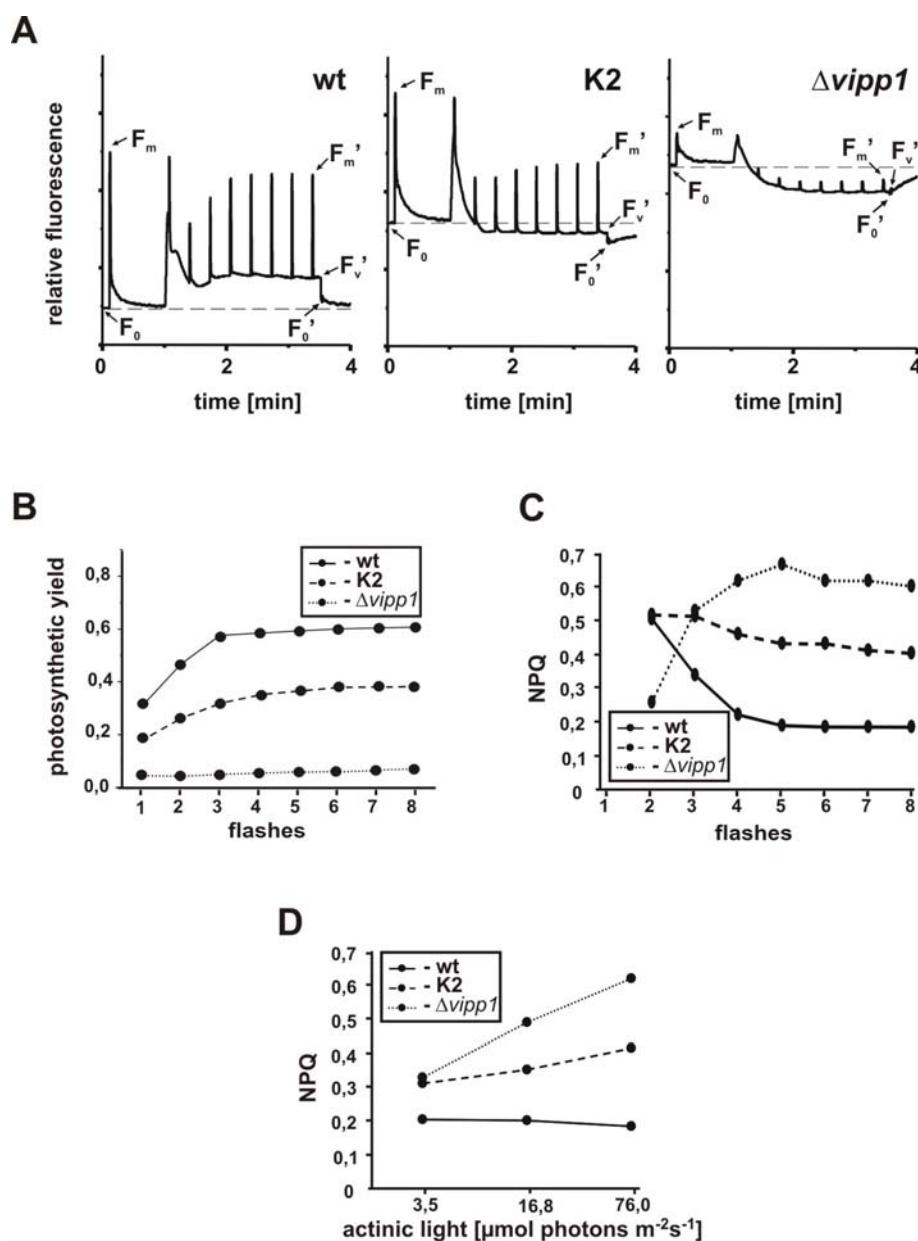
Figure 20: Comparison of the chlorophyll fluorescence induction kinetics in wild type (wt), K2 and Δ*vipp1* plants.

Actinic light was applied to dark adapted plants (F_0) and a saturating light flash of 4000 μmol photons m^{-2} s^{-1} was given in order to record maximal fluorescence (Fm). Consecutive pulses were given at intervals of 20 sec. F_0' designates the minimal fluorescence level after induction, Fm' is a maximal fluorescence level after induction. (A) Recording of the complete time course of a representative experiment performed with an actinic light intensity of 76.0 μmol photons m^{-2} s^{-1}. (B) Kinetics of the photosynthetic yield after induction were calculated from the experiment displayed in A. (C) Kinetics of NPQ after each consecutive pulse for plants illuminated with 76.0 μmol photons m^{-2}s^{-1} actinic light. (D) NPQ values after the last saturating pulse acquired for plants pre-illuminated with different intensities of actinic light ranging from 3.5 to 76.0 μmol photons m^{-2} s^{-1}.

wild type and the high level described for the *high chlorophyll fluorescence* phenotype of the $\Delta vipp1$ mutant (Fig. 20 A).

The kinetics of PSII activity during induction were recorded after each flash (Fig. 20 B) and they show that in K2 plants the PSII activity amounts to only about 60% of the wild type while in case of $\Delta vipp1$ the photosynthetic yield never exceeded more than 10% of the wild type level (Fig. 20 B). It was observed in the course of the experiment that K2 as well as $\Delta vipp1$ is characterized by an F_0' level that is below F_0 (Fig. 20 A). Therefore, the non-photochemical fluorescence quenching in these plants was estimated. The thermal dissipation processes referred to as non-photochemical quenching (NPQ) regulate photosynthesis when light energy absorption exceeds the capacity for light utilization.

Firstly, the level of NPQ was calculated after each flash in the experiment presented in figure 20 A. The NPQ of the wild type remained constant below a relative level of 0.2, indicating that the amount of actinic light used in this experiment is not sufficient to induce strong NPQ in the wild type. In contrast, $\Delta vipp1$ displayed an increase in NPQ by approx. 4 fold, while the NPQ of K2 plants appeared to be 2.5 times higher then in the wild type (Fig. 20 C). When the final level of NPQ was compared in correlation to different light intensities (3.5, 16.8 and 76.0 µmol photons $m^{-2}s^{-1}$), it was observed that the NPQ of $\Delta vipp1$ gradually rose under conditions of increasing light. The same effect was detected for K2 plants, although to lesser extent (Fig. 20 D), indicating that K2 plants cannot utilize the same amount of light energy as the wild type.

Finally the redox state of the PSI primary donor was analysed by determining the P700 absorption measured at 830 nm (Fig. 21). The relative ratio of the redox state of P700 was calculated for wild type, K2 and $\Delta vipp1$ plants pre-illuminated with actinic light of
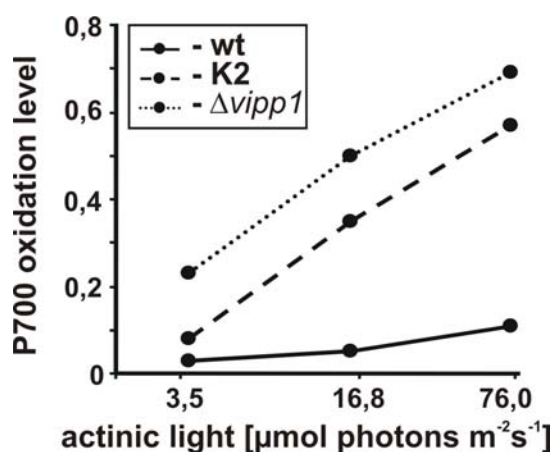

Figure 21: Analysis of the redox level of the PSI reaction center P700.

Measurements of P700 were performed at 830 nm as described in *Materials and Methods*. 3.5, 16.8 and 76.0 µmol photons $m^{-2}s^{-1}$ actinic light intensities were subsequently applied to the same sample. The redox level of PSI was determined as $\Delta A/\Delta A_{max}$.

different intensities (3.5, 16.8 and 76.0 µmol photons $m^{-2}s^{-1}$). The P700 oxidation level of Δ*vipp1* plants clearly exceeds that of the wild type both in low and in high light and it displays a distinct light dependency. A similar light dependency can be observed for K2 but not in the wild type plants, at least not to a comparable degree. While the PSI oxidation level of K2 is only slightly increased at low light, the difference to the wild type plants becomes more notable with increasing light intensities. This strong photosensitivity of the mutants is in agreement with the observation that Δ*vipp1* but also K2 plants grow much better under low light. Thus, expression of the Vipp1-protA fusion protein only partially restored the photosynthetic activity, which is strongly impaired in the original Δ*vipp1* mutant.

6.3.3. Analysis of Vipp1 protein level and complex assembly in K2 and Δ*vipp1* plants

The analysis above suggests that while the Vipp1-ProtA fusion protein is principally able to substitute for Vipp1, the amount of functional Vipp1 protein produced by K2 plants is not adequate to fully restore the wild type phenotype under high light conditions. It could be either due to a limitation in expression of the Vipp1-ProtA fusion protein or because of a restricted functionality of the Vipp1-ProtA fusion protein. To address this question, the level of Vipp1-ProtA produced in the K2 plants was analysed by Western blot in comparison to the Vipp1 content in both wild type and Δ*vipp1* plants. In the original Δ*vipp1* mutant, the Vipp1 content is drastically reduced to less than 20% compared to the wild type level. A similar level of Vipp1 protein is also found in the K2 plants, as visible from the faint band at about 33 kDa (Fig. 22 A, left panel). Additionally, the K2 plants contain about equal amounts of the Vipp1-ProtA fusion protein as evident from the immunoreaction at 42 kDa. This protein is also immunodecorated with an IgG specific secondary antibody (Fig. 22 A, right panel). Neither the wild type plants nor the original mutant show any immunoreaction in this position, indicating that it is indeed Vipp1-ProtA fusion protein (Fig. 22 A, right panel). Nevertheless, even Vipp1 and Vipp1-ProtA together amount to not more than approximately 40% of the wild type level of Vipp1 protein (Fig. 22 A, left panel). Therefore, the observed phenotype of K2 could be ascribed to a reduction in the overall content of Vipp1 protein.

In chloroplasts as well as cyanobacteria a significant amount of Vipp1 protein is found as part of a homo-multimeric complex of approx. 2000 kDa (see Fig. 7). To test whether Vipp1-ProtA fusion protein preserves the ability to assemble into a complex, the presence

of this complex was investigated in K2 and compared with wild type and Δ*vipp1* plants
(Fig. 22 B). For this analysis, total membranes from wild type, K2 and the original Δ*vipp1*

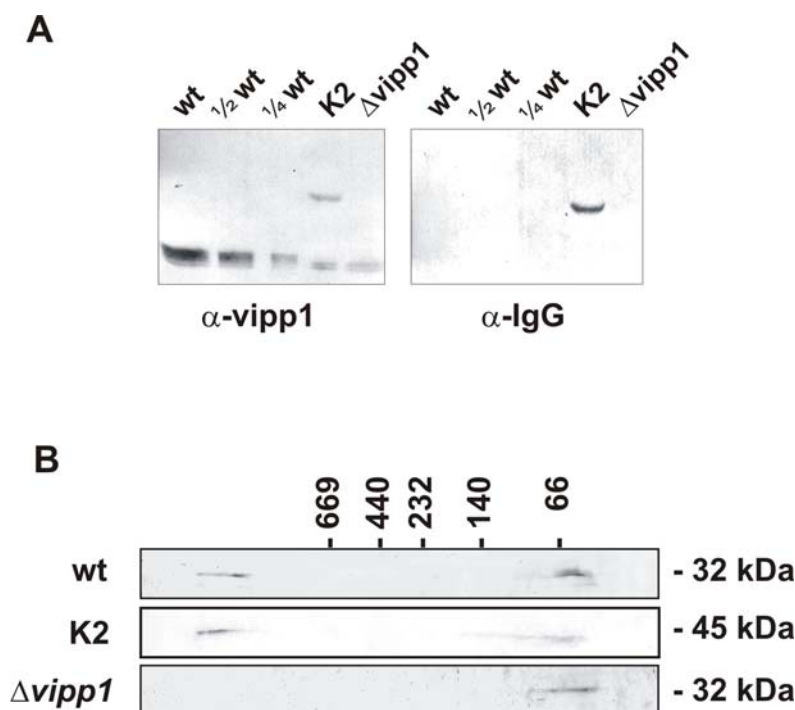**Figure 22: Analysis of Vipp1 in wild type, K2 and Δ*vipp1* plants.**

(A) Immunodecoration of the Vipp1 protein in total leaf extracts of wild type (wt), K2 and Δ*vipp1* plants. Equal amounts of fresh weight tissue were used in sample preparation and subsequently equal sample volumes were loaded. In case of the wild type 50% and 25% of the original sample volume (½ wt and ¼ wt, respectively) was loaded additionally. Endogenous as well as Vipp1-ProtA fusion protein was detected with the α-Vipp1 antibody (left panel). Additionally, the Vipp1-ProtA fusion protein in the K2 plants was detected with a secondary antibody (right panel), which recognizes the IgG-binding domain of ProteinA. (B) Analysis of complex formation by Vipp1 and Vipp1-ProtA in wild type (wt), K2 and Δ*vipp1* plants. Proteins from total membrane fractions separated first by BN-PAGE and subsequently by SDS-PAGE were immunodecorated with α-Vipp1 antibody. Immunoreaction with Vipp1 is found in a position corresponding either to the complex (>1000 kDa) or the monomeric form of Vipp1.

mutant were separated first on BN- and then on SDS-PAGE, followed by Western blot analysis using an α-Vipp1 antiserum. In order to achieve a visible immunoreactive band, double amount of material by fresh weight from Δ*vipp1* plants was loaded onto the BN-

PAGE in comparison to wild type and K2. The Western blot analysis showed very little difference between wild type and K2 plants. In both cases, two immunoreactive bands could be detected, corresponding to the monomeric and the complex form of the protein (Fig. 22 B, first and second panel). The fact that the Vipp1-ProtA fusion protein is found in both positions indicates that the phenotype of K2 plants is not caused by an inability of the Vipp1-ProtA fusion protein to assemble into a high molecular weight complex. Surprisingly, when the Δ*vipp1* mutant was subjected to this analysis, the residual Vipp1 present in these plants was found exclusively in the monomeric state (Fig. 22 B, lower panel). It cannot be excluded that the Vipp1 complex in this mutant is much less stable and, therefore, dissociates during the preparation. Nevertheless, it seems more likely that due to the lack of critical mass of Vipp1 protein no complex is formed in the mutant. This would imply that complex formation of the Vipp1 protein is subject to a dose effect, which is quite likely since a single Vipp1 complex comprises many Vipp1 molecules.

6.3.4. Content and assembly status of thylakoid proteins in Δ*vipp1* and K2 plants

Previous analysis of the Δ*vipp1* mutant could not determine whether Vipp1 functions in the biogenesis of the thylakoid membrane itself or in the assembly of functional membranes. Due to its albinotic phenotype the original Δ*vipp1* mutant suffered from a number of secondary defects not directly connected to the loss of Vipp1. Since the *VIPP1-PROTA* insertion re-established autotrophic growth and partially restored the photosynthetic activity of the plants in the background of moderate Vipp1 deficiency, it allowed for elucidating the primary effects that Vipp1 shortage has on the development of the thylakoid system. To investigate whether Vipp1 deficiency has an effect on the principal complex assembly at the thylakoid membrane, the content and assembly status of photosynthetic complexes in the thylakoid membrane of K2 and Δ*vipp1* were elucidated.

First, total leaf samples of wild type, K2 and Δ*vipp1* plants were analysed in Western blotting for the presence and relative amount of several thylakoid membrane proteins, including several components of the photosynthetic apparatus as well as the ATP synthase. Additionally, some proteins of the inner envelope membrane were analysed, which are not directly related to the photosynthetic process. The comparison was based on equal fresh tissue weight used in sample preparation. Western blot analysis revealed that different proteins were affected to varying degrees in the mutant plants (Fig. 23). All PSII proteins analysed were reduced to about 20-30% of the wild type level in K2 plants. A similar

reduction could be observed for the PSII assembly factor HCF136, for Cytf, LHCB1 and for the PSI core subunit PsaD. In case of the chloroplast ATP synthase subunits, the K2 plants contained at least 50% of the protein levels compared to the wild type, in some cases even significantly less. In comparison, levels of photosynthetic protein in Δ*vipp1* plants were much more drastically reduced and often constitute not more then 10% of the wild type level (Fig. 23). The amount of LHCB1 protein in the Δ*vipp1* plants appears rather high for a mutant nearly devoid of thylakoid membranes but this is in accordance with spectroscopic studies indicating the presence of free LHCII-trimers (compare Fig. 19).
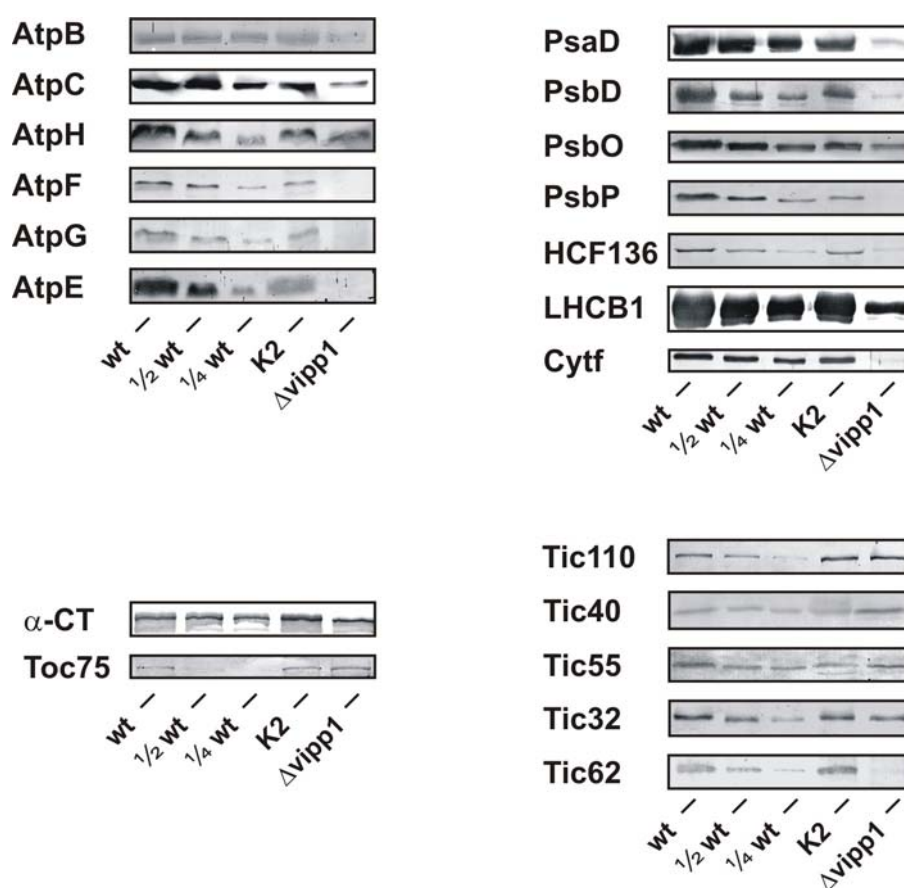

Figure 23: Analysis of the chloroplast protein content of in K2 and Δ*vipp1* plants.
Total leaf extracts of wild type (wt), K2 and Δ*vipp1* plants were separated by SDS-PAGE, blotted and immunodecorated with the indicated antisera. Equal amounts of fresh weight tissue were used in sample preparation and subsequently equal sample volumes were loaded. In case of the wild type 50% and 25% of the original sample volume (½ wt and ¼ wt, respectively) was loaded additionally.

However, the level of proteins not involved in the photosynthetic process, such as the α-subunit of the acetyl-CoA carboxyltransferase (α-CT), was not significantly altered in K2 or in Δ*vipp1* (Fig. 23). Similarly, no significant changes in the protein amount were detected for most of the Toc and Tic import apparatus components, with the exception of Tic62 (Fig. 23 and data not shown). Some components of the Tic machinery, such as the protein import subunit Tic110, even displayed an increase in the Vipp1-deficient plants.

Thus, the observed reduction in the photosynthetic proteins is not due to the overall reduction in the protein content in K2 and Δ*vipp1* plants but represents a specific effect of Vipp1 deficiency. Interestingly, while no reduction of Tic62 could be observed in K2 plants, the level of Tic 62 in Δ*vipp1* mutant is decreased to less then 20%, when compared to wild type. Since Tic62 was shown to interact with FNR (Kuchler et al., 2002), which is sensitive to the chloroplast redox state (Pfannschmidt et al., 2001), one could assume that decrease in Tic62 might be a result of the redox signalling used by the chloroplast to modulate import activity.
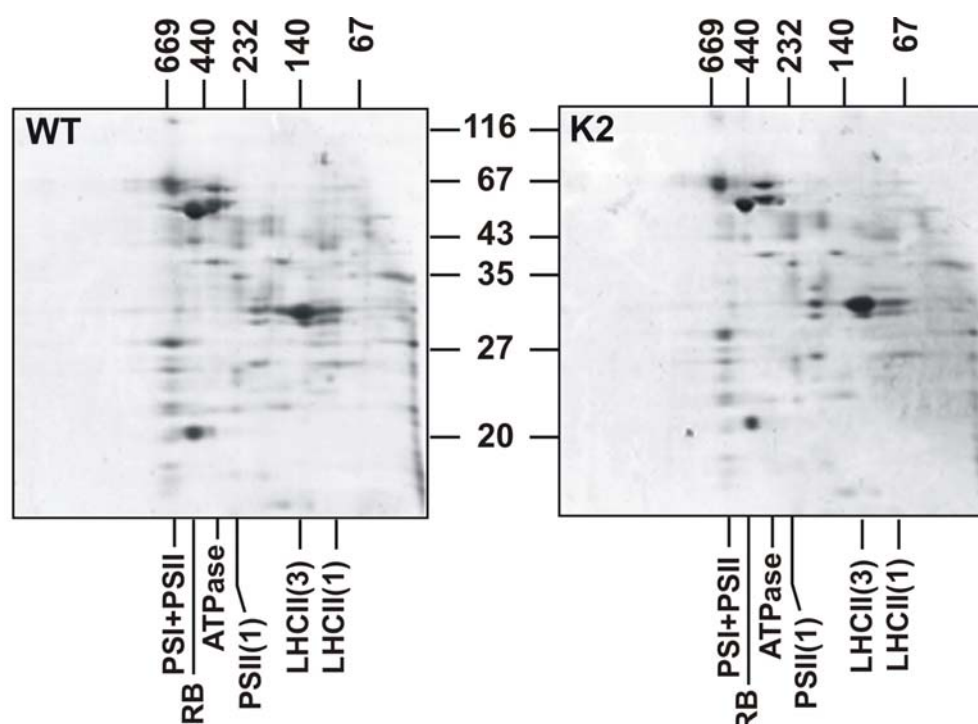

Figure 24: Analysis of assembly of photosynthetic complexes in wild type (wt) and K2 chloroplasts.
Chloroplasts were isolated and protein complexes were separated on BN-PAGE in the first and SDS-PAGE in the second dimension. Proteins were visualized by staining with Coomassie Brillant Blue.

The assembly status of photosynthetic complexes was analysed in wild type and K2 chloroplasts separated first under native and then under denaturing conditions (Fig. 24). Taking into consideration a lower protein level of photosynthetic components in K2 compared to wild type, double the amount of the K2 fresh leaf tissue was used in sample preparation. Δ*vipp1* was excluded from this analysis due to its overall low protein content, which makes it very difficult to detect the proteins in this type of analysis. The comparison of K2 with wild type did not reveal any discernable difference in the assembly status of the photosynthetic complexes (Fig. 24). The overall picture obtained from this analysis rather indicates that deficiency in Vipp1 results in a correlated shortage of photosynthetic proteins with very little direct impact on the assembly of the photosystems.

6.3.5. Chloroplast ultrastructure of K2 plants

To elucidate to which extent the K2 plants are affected in thylakoid formation, the ultrastructure of the K2 chloroplasts was studied by transmission electron microscopy. In leaf tissue of K2 plants, chloroplasts at very different stages of thylakoid development could be observed simultaneously in one and the same cell (Fig. 25 a to e). Figure 25 a and b show typical examples of this situation with one chloroplast very much resembling wild type (Fig. 25 g) and the neighboring plastid nearly devoid of internal membranes, and therefore similar to the original Δ*vipp1* mutant (Fig. 25 f).

Further examination of several different thin sections of K2 plants revealed a wide representation of plastids as displayed in figure 25 c to e. While many of them contain an elaborate thylakoid membrane system with extensive grana stacking, other plastids encompass only partially formed thylakoid systems. In some cases, properly stacked thylakoids are restricted to the periphery of the organelle but are not found in its center (Fig. 25 e). The residual membranes found in many of these chloroplasts appear to assemble from centers inside the organelle in a fashion not unlike the formation of thylakoids from prolamellar bodies when chloroplasts develop from etioplasts (Fig. 25 c). It appears that partial Vipp1 deficiency has the unusual consequence that some of the plastids can achieve a normal development while others are arrested in various stages of completion of thylakoid formation.
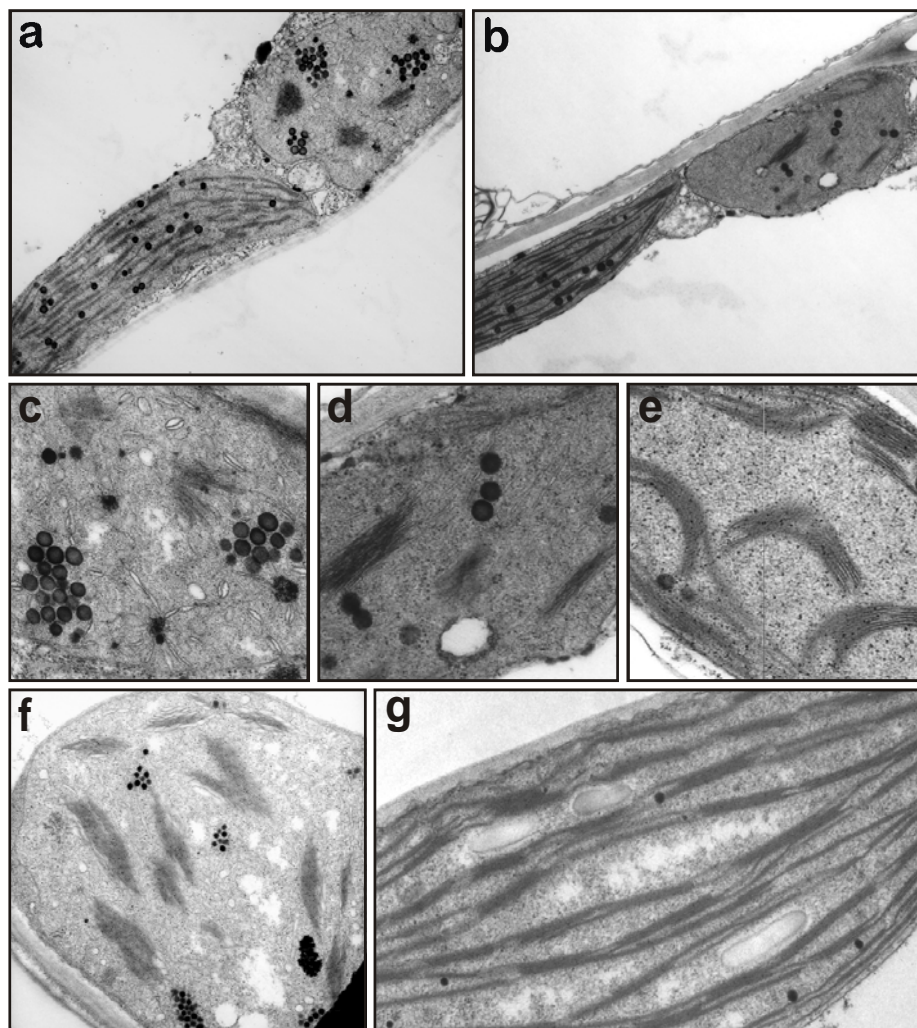
Figure 25: Electron microscopic analysis of the ultrastructure of K2 chloroplasts.
(a) and (b) representative electron micrographs of K2 plants with differently chloroplasts in one and the same cell; (c) to (e) enlargement of different chloroplasts found in K2 plants; (f) typical chloroplast found in the Δ*vipp1* mutant; (g) typical wild type chloroplast.

6.3.6. Expression of Vipp1-GFP fusion protein in Δ*vipp1* mutant protoplasts

The data obtained in the Western blotting analysis show that the level of photosynthetic proteins in Δ*vipp1* mutant is drastically decreased. Moreover, the residual Vipp1 in Δ*vipp1* mutant was found only in the monomeric form, either due to instability of the Vipp1 complex or due to insufficient amount of Vipp1 molecules to form detectable numbers of

complexes. At the same time, the components of the chloroplast import machinery in Δ*vipp1* were present on the level comparable with wild type, with the only exception of Tic62, which was found to be highly reduced. These data, however, do not provide us with information about the functionality of the import apparatus in Δ*vipp1*. It is also not clear whether the ability of Vipp1 to attain proper localization at the inner envelope membrane of chloroplasts is preserved in these mutants.

This question was approached by means of GFP-fusion technique. Protoplasts isolated from wild type and Δ*vipp1 Arabidopsis* plants were transformed with the construct Vipp1-GFP fusion as described in **6.2.7.** Changes in the pattern of chlorophyll fluorescence could be observed between the protoplasts of wild type and Δ*vipp*1. In general, the thylakoids of wild type chloroplasts are visible in discrete dots, indicating positioning of grana stacks (Fig. 26 a). In Δ*vipp1*, the distribution of chlorophyll fluorescence is more homogenous (Fig. 26 b) and the intensity of the fluorescence signal is low (data not shown). Some chloroplasts do not exhibit any detectable chlorophyll fluorescence signal at all. Also the area displaying the chlorophyll fluorescence signal is generally smaller than in wild type and more restricted to the center of chloroplasts (Fig. 26 b). This phenomenon was earlier observed in a number of mutants with impaired thylakoid system. As described in **6.2.7.**, transformation of *Arabidopsis* or tobacco wild type protoplasts with Vipp1-GFP construct revealed a GFP-fluorescence signal in distinct locations at the chloroplast inner envelope. When protoplasts isolated from Δ*vipp1* were transformed with the same construct, a similar pattern of GFP-fluorescence was observed (Fig. 26 c). Namely, Vipp1-GFP was found in a ring-like arrangement consisting of distinct spots emulating the shape of the chloroplasts, as it is demonstrated by overlaying the transmission and GFP-fluorescence images (Fig. 26 e). No Vipp1-GFP could be detected colocalized with chlorophyll autofluorescence (Fig. 26 f), i.e. with the residual thylakoid membrane. Moreover, the Vipp1-GFP signal could be found in mutant chloroplasts whether they exhibited chlorophyll autofluorescence or not.
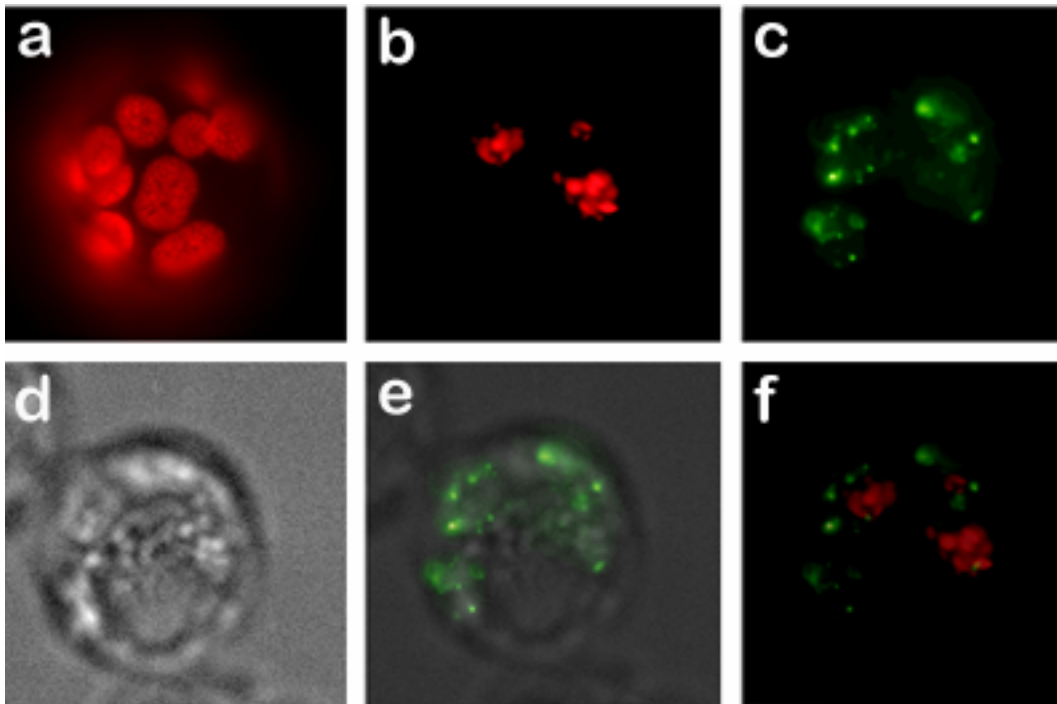
Figure 26: Transformation of Δ*vipp1* protoplasts with Vipp1-GFP fusion construct.
a, Chlorophyll fluorescence of a typical wild type protoplast. b-f, Expression of Vipp1-GFP in Δ*vipp1* protoplasts. b, Chlorophyll fluorescence of Δ*vipp1* mutant; c, GFP-fluorescence; d, transmission; e, overlay of transmission and GFP-fluorescence; f, overlay of chlorophyll and GFP-fluorescence.

Thus, the GFP-fusion approach shows that Δ*vipp1* plants are capable of importing Vipp1 into the chloroplasts. The Vipp1-GFP fluorescence pattern was identical to wild type, indicating that potentially the ability of Vipp1 to attain proper localization is maintained in the Δ*vipp1* mutant.

7. Discussion

Despite the obvious importance of the thylakoid system for the photosynthetic process, only very little is known about the components involved in the biosynthesis of the thylakoid membrane. Analysis of Δ*vipp1* mutants of *Arabidopsis* and *Synechocystis* provided first indications that the Vipp1 protein plays an essential role in thylakoid formation. These mutants were characterized by an almost complete loss of their thylakoid membrane system (Kroll et al., 2001; Westphal et al., 2001a). Initial characterization of the photosynthetic activity in the Δ*vipp1 Arabidopsis* plants did not reveal any specific effects on the photosynthetic process but rather suggested its general distortion. Remarkably, in *Arabidopsis* Δ*vipp1* plants, the loss of the thylakoid system was accompanied by the loss of vesicles in the stroma of chloroplasts (Kroll et al., 2001), which can be interpreted as an inability of the chloroplast to give rise to new membranes under conditions of Vipp1 deficiency. However, the exact role of Vipp1 in the process of the thylakoid development remained enigmatic, and this work was performed in order to provide further knowledge about the function of this protein. Firstly, the structure of the Vipp1 protein was studied in detail, in order to get an insight into the mechanism of its action. This structural approach was complemented by the analysis of *Arabidopsis* plants with a less severe Vipp1 deficiency, which was performed in attempt to discern the primary effects that limitation of Vipp1 has on the thylakoid membrane.

When Vipp1 was first identified as a protein associated with the inner envelope and the thylakoid membrane in the chloroplasts of *Pisum sativum*, BLAST analysis revealed its similarity to a bacterial protein, PspA, that is essential for membrane integrity under many stress conditions (Li et al., 1994). Phylogenetic analysis further indicated that these two proteins are homologous and that Vipp1 originated from PspA (Westphal et al., 2001a). The region homologous to PspA covers about 70% of the Vipp1 sequence (PspA-like domain). However, these two proteins differ by the presence of an additional C-terminal extension acquired by Vipp1, which is believed to be important for its novel function in thylakoid biogenesis.

In this work it is shown that Vipp1 forms a high molecular weight complex composed of multiple copies of the protein and located at the inner envelope membrane of chloroplasts and the plasma membrane of cyanobacteria. At about the time this finding was made, assembly in a large multimeric complex was also demonstrated for PspA from
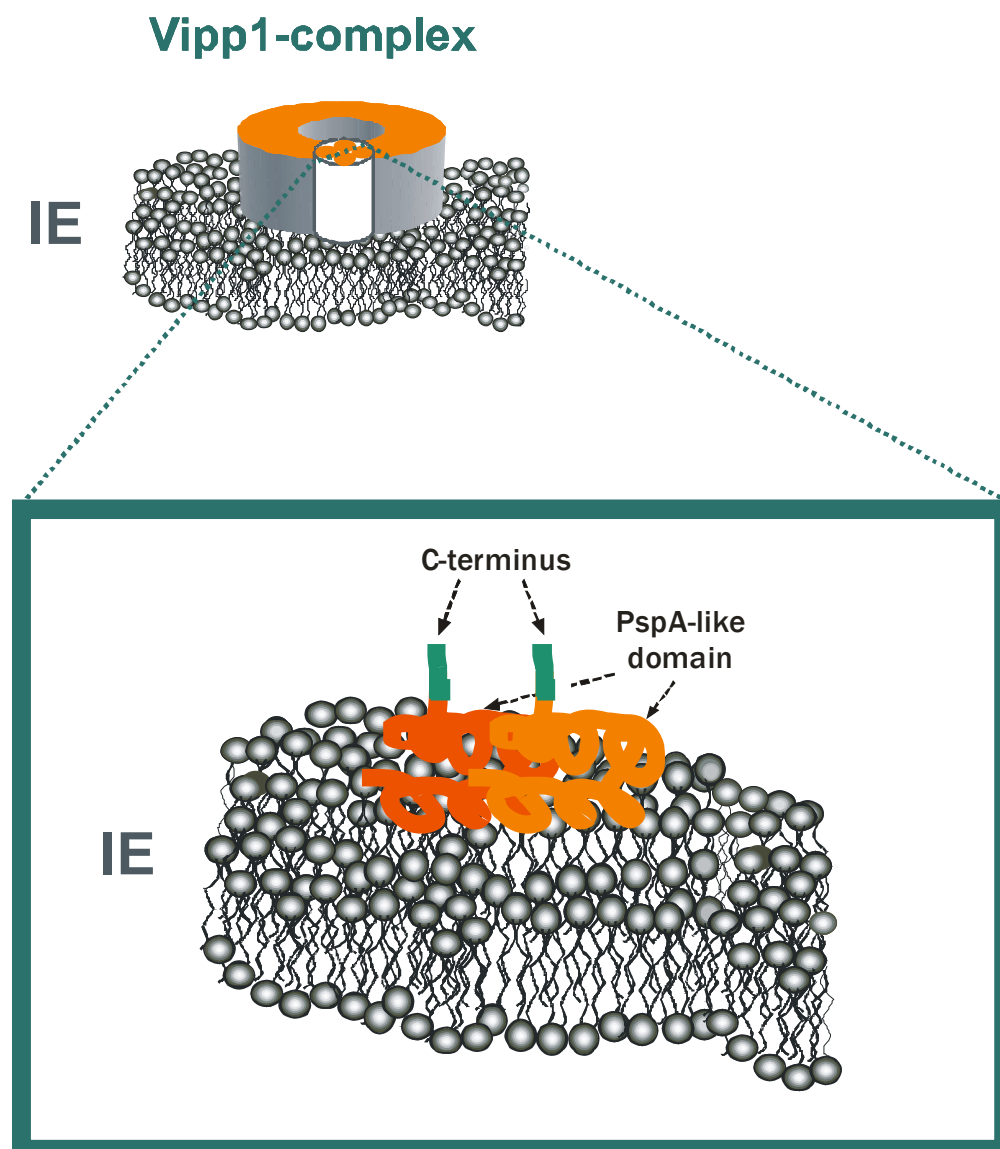
Figure 27: A current model for the structure of the Vipp1 complex and its localization at the inner envelope membrane of chloroplasts.

The complex is organized in a ring-like structure consisting of Vipp1-tetramers formed by two Vipp1-dimers. The interaction of subunits within the complex is schematically represented at an example for a Vipp1-dimer. PspA-like domains of two Vipp1 proteins interact with each other. These domains are also responsible for the membrane association of the complex. The C-terminal domain is not involved in this kind of interactions and protrudes out of the complex.

E. coli (Hankamer et al., 2004). Likewise as Vipp1, the PspA complex is made of many copies of PspA and a minimal unit in the complex assembly is represented by homodimers.

Both, Vipp1 and PspA complexes are ring-shaped structures of similar appearance, even though different in size. Remarkably, more detailed analysis of the Vipp1-complex showed that its formation is carried out by the PspA-like domain. Whereas removal of the C-terminal part of Vipp1 did not have an effect on its assembly into a multimeric complex, the disruption of the PspA-like domain prevented the complex formation, and Vipp1 could be detected only in a monomeric form.

This finding further accentuates the similarity between complexes build up by PspA and Vipp1. Such resemblance poses the question whether the function of the two proteins, although undoubtedly different in terms of its application and regulation, is based on similar principles of action. Experimental data demonstrate that at least under certain conditions Vipp1 is able to take over the function of PspA. In the recent work of DeLisa and co-workers (DeLisa et al., 2004) overexpression of Vipp1 from *Synechocystis* could substitute PspA in relieving blockage of the Tat pathway in *E. coli*. On the other hand, disruption of the *VIPP1* gene in *Synechocystis* results in drastic effects on the thylakoid formation despite the presence of the functional *PSPA* (Westphal et al., 2001a), supporting the importance of the C-terminal domain for the function of Vipp1. However, the role of this Vipp1-specific C-terminus so far remains elusive. Computer analysis shows a comparatively low amino acid similarity of this domain between Vipp1 proteins from different organisms. Nevertheless, its secondary structure is always preserved and therefore is apparently important: in all Vipp1 proteins analysed, the C-terminal extension constitutes a random coil region followed by a short α-helix. Moreover, characteristics of this structure can be used for differentiating Vipp1 from PspA proteins with prolonged C-termini. Yet, the data accumulated up to the present rather rule out a direct involvement of this C-terminal extension in processes such as Vipp1 complex formation and its localization at the inner envelope membrane of chloroplasts. It seems more likely that these processes are carried out in an "old-fashioned" PspA-like manner, whereas the additional C-terminal domain serves the novel function of Vipp1 in the thylakoid biogenesis. The data presented in this work indicate that the C-terminus is not buried inside the Vipp1 complex but rather protrudes out of it, which potentially enables it to interact with other partners involved in biogenesis of thylakoids. The question of how exactly the Vipp1 molecule is orientated within the complex requires further experimental analysis. So far it is not clear whether the C-terminal part is directed toward the inner or the outer surface of the Vipp1-ring. A presence on both sides of the complex is also not excluded. Our current

knowledge about the structure of the Vipp1 complex is schematically presented in figure 27.

As mentioned above, Vipp1 complex formation and membrane localization are dependent on the PspA-like domain of Vipp1. More precisely, the central, fourth α-helix of the protein is required for both processes. So far it is not clear whether the complex assembly precedes its localization at the membrane or if both processes occur simultaneously. More detailed analysis of the domain architecture is required to clarify this question. It is important to notice that attachment of PspA to the membrane is mediated via its interactions with two other members of the *psp* operon, PspB and PspC. Interestingly, no homologues of these proteins are found either in *Synechocystis* or in *Arabidopsis* genomes. Another clear difference is that PspA is present in both a soluble and membrane-bound pool, while Vipp1, according to the data obtained in our laboratory, is most likely constantly attached to the membrane. It is tempting to explain this distinction by a different mode of regulation of these two proteins. The necessity of different regulation becomes apparent when we compare what is known about the functions of PspA and Vipp1. PspA plays a crucial role in protecting the bacterial membrane from stress-inducible alterations, and the function of PspA becomes critical only when membrane integrity is in danger. Consistently, *pspA* mutants do not exhibit a distinct phenotype under normal conditions but show incapability of coping with conditions leading to decrease or dissipation of the proton motive force (Kleerebezem and Tommassen, 1993). Under these conditions, PspA is recruited from a soluble pool to the bacterial membrane in a process mediated by interactions with transmembrane proteins PspB and PspC. Once the stress is over, PspA is no longer needed at the membrane and is dispersed to the cytoplasm. In contrast, involvement of Vipp1 in the process of thylakoid development, i.e. an ongoing process of formation of a novel membrane, could explain the need of its permanent presence at the inner envelope. One can assume that in this case the "shuttling"-type regulation applied for PspA becomes superfluous. Instead, more stable interaction of Vipp1 with the inner envelope membrane is required. Yet, how exactly Vipp1 conducts this interaction remains to be studied. Until now, no interactions of Vipp1 with transmembrane proteins, potential candidates for this role, could be identified. It is furthermore intriguing to speculate that Vipp1 may attach itself to the membrane via direct interaction with the membrane bilayer.

So, what is the function of Vipp1 in the thylakoid biogenesis? The analysis of *Arabidopsis* plants with moderate deficiency in Vipp1 protein (K2) and their comparison

with the original Δ*vipp1* mutant strongly supports the previous supposition that Vipp1 acts very early in thylakoid development and is needed basically for the formation of the thylakoid membrane per se. The content of photosynthetic proteins in K2 and Δ*vipp1* is diminished proportionally to the overall amount of the thylakoid membrane built up by the chloroplasts of these plants, and analysis of the assembly state of the photosynthetic complexes did not reveal any considerable difference between K2 and wild type. Thus, it seems that the degree of the thylakoid membrane formation is the key factor for the amount of the photosynthetic machinery assembled under conditions of Vipp1 deficiency. Furthermore, the function of Vipp1 in this process appeared to be dosage-dependent, as follows from a comparison of the phenotypes of plants with different degrees of Vipp1 deficiency. While the Δ*vipp1* mutants are able to grow only heterotrophically, the Vipp1-ProtA insertion restores autotrophic growth. However, there is a clear phenotypic difference between homozygous and heterozygous Vipp1-ProtA plants, and the amount of Vipp1 produced by heterozygous (K2) plants seems to be insufficient to fully restore thylakoid formation. Instead, the K2 plants contain chloroplasts at different stages of thylakoid development in one and the same cell. This finding by itself is extremely unusual as an effect caused by deficiency of a nuclear encoded protein. If the amount of Vipp1-ProtA is the only determining factor for the degree of thylakoid membrane formation in K2 plants, we have to assume that the Vipp1-ProtA fusion protein is unequally distributed into the plastids of a cell. One can suppose that if the overall amount of Vipp1 produced by K2 plants represents the threshold level with regard to its function, even slight differences in distribution of Vipp1 between the chloroplasts may have drastic influence on the thylakoid development. This would be consistent with the observation that under lower light, i.e. under conditions of slower growth, a reduced Vipp1 function is sufficient, while under high light conditions Vipp1 function becomes more easily limiting and the tissue becomes albinotic. Interestingly, although K2 plants support Vipp1 complex formation, stronger reduction of Vipp1 content in the case of Δ*vipp1* plants seems to prevent the assembly of the residual Vipp1 protein into a complex. Bearing in mind how many Vipp1 molecules are needed to form one functional complex, this phenomenon can be regarded as another manifestation of a dose effect and may well account for the more drastic phenotype of Δ*vipp1* comparing to K2 plants.

All in all, the analysis performed in this work reveals an essential role of Vipp1 in the formation of the thylakoid system. Future studies will have to disclose an exact mechanism

of Vipp1 action at the membrane. First of all, detailed analyses of the Vipp1 domain architecture is required to provide information about subdomains and particular amino acids responsible for oligomerisation of Vipp1, and to reconstruct the sequence of events leading to the Vipp1 complex formation. Moreover, it may help to answer the question which additional factors are required for the attachment of the Vipp1 complex to the membrane. These factors may include protein components serving as mediators for membrane association as well as lipid components in the case that Vipp1 interacts with the lipid bilayer directly. In a search for Vipp1 interacting proteins performed in our laboratory, we identified a chloroplast chaperone cpHsp70B (At4g24280). The interaction of Vipp1 with Hsp70B was independently confirmed in the work of Liu et al. (2005). The authors found Vipp1 as a binding partner for Hsp70B/CDJ2 chaperone pair of *Chlamydomonas reinhardtii* chloroplasts. It is proposed that interaction of CDJ2 and subsequently Hsp70B with Vipp1 is needed for assembly/disassembly of Vipp1 oligomers. Our data further indicate that this interaction takes place at the Vipp1 specific C-terminus.

The role of the Vipp1 C-terminal domain remains the most intriguing subject of research. It seems unlikely that the function of this evolutionary important acquisition is restricted to the interaction with chaperones and regulation of the Vipp1 complex assembly, given that our experiments indicate dispensability of the C-terminus for Vipp1 oligomerization. Future investigation will have to unveil the function of the Vipp1 C-terminal domain and answer the central question: "what does make Vipp1 indispensable for the thylakoid formation?"

8. References

Allen, J.F. (1992) Protein phosphorylation in regulation of photosynthesis. Biochim. Biophys. Acta, 1098, 275−335.

Allen, J.F., Forsberg, J. (2001) Molecular recognition in thylakoid structure and function. Trends Plant Sci., 6, 317-326.

Albertsson, P. (2001) A quantitative model of the domain structure of the photosynthetic membrane. Trends Plant Sci., 6,349-358.

Anderson, J.M. (1986) Photoregulation of the composition, function and structure of thylakoid membranes. Annu. Rev. Plant Physiol. Plant Mol. Biol., 37, 93–136.

Andersson, B. and Anderson, J.M. (1980) Lateral heterogeneity in the distribution of chlorophyll–protein complexes of the thylakoid membranes of spinach chloroplasts. Biochim. Biophys. Acta, 593, 427–440.

Arnon, D.J. (1949) Copper enzymes in isolated chloroplasts. Polyphenoloxidase in *Beta vulgaris*. Plant Physiology, 24, 42-45.

Bellafiore, S., Barneche, F., Peltier, G., Rochaix, J.D. (2005) State transitions and light adaptation require chloroplast thylakoid protein kinase STN7. Nature, 433, 892-895.

Bergler, H., Abraham, D., Aschauer, H., Turnowsky, F. (1994) Inhibition of lipid biosynthesis induces the expression of the pspA gene. Microbiology, 140, 1937-1944.

Bhattacharya, D. and Medlin, L. (1998) Algal Phylogeny and the Origin of Land Plants. Plant Physiol., 116, 9-15.

Bölter, B., May, T. and Soll, J. (1998) A protein import receptor in pea chloroplasts, Toc86, is only a proteolytic fragment of a larger polypeptide. FEBS Lett., 441, 59-62.

Block, M.A, Dorne, A.J, Joyard, J., Douce, R. (1983) Preparation and characterization of membrane fractions enriched in outer and inner envelope membranes from spinach chloroplasts. 11. Biochemical characterization. J. Biol. Chem., 258, 13281–13286.

Brissette, J.L., Russel, M., Weiner, L., Model, P. (1990) Phage-shock protein, a stress protein of *Escherichia coli*. Proc. Natl. Acad. Sci. USA, 87, 862-866.

Brissette, J.L., Weiner, L., Ripmaster, T.L., Model, P. (1991) Characterization and sequence of the *Escherichia coli* stress-induced *psp* operon. J. Mol. Biol., 220, 35-48.

Combet, C., Blanchet, C., Geourjon, C., Deléage, G. (2000) NPS@: Network Protein Sequence Analysis TIBS, 3, 147-150.

Cuff, J.A. and Barton, G.J. (2000) Application of multiple sequence alignment profiles to improve protein secondary structure prediction. Proteins, 40, 502-511.

Dekker, J.P. and Boekema, E.J. (2005) Supramolecular organization of thylakoid membrane proteins in green plants. Biochim. Biophys. Acta, 1706, 12-39.

DeLisa, M.P., Lee, P., Palmer, T., Georgiou, G. (2004) Phage shock protein PspA of *Escherichia coli* relieves saturation of protein export via the Tat pathway. J. Bacteriol., 186, 366-373.

Depege, N., Bellafiore, S. and Rochaix, J.D. (2003) Role of chloroplast protein kinase Stt7 in LHCII phosphorylation and state transition in Chlamydomonas. Science, 299, 1572-1575.

Dilley, R.A., Nishiyama, Y., Gombos, Z., Murata, N. (2001) Bioenergetic responses of Synechocystis 6803 fatty acid desaturase mutants at low temperatures. J. Bioenerg. Biomembr. 33, 135-141.

Douce, R. and Joyard, J. (1996) Advances in Photosynthesis, Vol. 4, Kluwer Academic Publishers, Dordrecht, 69-101.

Dworkin, J., Jovanovic, G. and Model, P. (2000) The PspA protein of *Escherichia coli* is a negative regulator of σ^{54}-dependent transcription. J. Bacteriol., 182, 311-319.

Elderkin, S., Bordes, P., Jones, S., Rappas, M., Buck, M. (2005) Molecular determinants for PspA-mediated repression of the AAA transcriptional activator PspF. J Bacteriol., 187, 3238-3248.

Elderkin, S., Jones, S., Schumacher, J., Studholme, D., Buck, M. (2002) Mechanism of action of the Escherichia coli phage shock protein PspA in repression of the AAA family transcription factor PspF. J Mol Biol., 320, 23-37.

Fincher, V., Dabney-Smith, C. and Cline, K. (2003) Functional assembly of thylakoid ΔpH-dependent/Tat protein transport pathway components *in vitro*. Eur. J. Biochem., 270, 4930-4941.

Gamborg, O.L., Murashige, T., Thorpe, T.A., Vasil, I.K. (1976) Plant tissue culture media. In Vitro, 12, 473–478.

Gorman, D.S. and Levine, R.P. (1965). Cytochrome f and plastocyanin, their sequence in the photosynthetic electron transport chain of *Chlamydomonas reinhardii*. Proc. Natl. Acad. Sci. USA, 54, 1665–1669.

Hankamer, B.D., Elderkin, S.L., Buck, M., Nield, J. (2004) Organization of the AAA(+) adaptor protein PspA is an oligomeric ring. J Biol Chem., 279, 8862-8866.

Hardie, K.R., Lory, S. and Pugsley, A.P. (1996) Insertion of an outer membrane protein in Escherichia coli requires a chaperone-like protein. EMBO J., 15, 978-988.

Hoober, J., Boyd, C.O. and Paavola, L.G. (1991) Origin of Thylakoid Membranes in *Chlamydomonas reinhardtii y-1* at 38°C. Plant Physiol., 96, 1321–1328.

Hoober, J.K. and Eggink, L.L. (2001) A potential role of chlorophylls b and c in assembly of light-harvesting complexes. FEBS Lett., 489, 1-3.

Horton, P. (1999) Are grana necessary for regulation of light harvesting? Aust. J. Plant Physiol., 26, 659–669.

Huang, F., Parmry, I., Nilsson, F., Persson, A.L., Pakrasi, H.B., Andersson, B., Norling, B. (2002) Proteomics of *Synechocystis* sp. strain PCC 6803. Mol. Cell. Proteomics, 1, 956.

Joliot, P., Beal, D. and Joliot, A. (2004) Cyclic electron flow under saturating excitation of dark-adapted Arabidopsis leaves. Biochim Biophys Acta, 1656,166-176.

Joliot, P. and Joliot, A. (2002) Cyclic electron transfer in plant leaf. Proc Natl Acad Sci USA, 99, 10209-10214.

Jones, S.E., Lloyd, L.J., Tan, K.K., Buck, M. (2003) Secretion defects that activate the phage shock response of *Escherichia coli.* J. Bacteriol., 185, 6707-6711.

Jovanovic, G. and Model, P. (1997) PspF and IHF bind co-operatively in the psp promoter-regulatory region of Escherichia coli. Mol Microbiol., 25, 473-481.

Jovanovic, G., Weiner, L., Model, P. (1996) Identification, nucleotide sequence, and characterization of PspF, the transcriptional activator of the *Escherichia coli* stress-induced *psp* operon. J. Bacteriol., 178, 1936-1945.

Keegstra, K. and Youssif, A.E. (1986) Isolation and characterization of chloroplast envelope membranes. Methods Enzymol., 118, 316-325.

Kelly, A.A. and Dormann, P. (2004) Green light for galactolipid trafficking. Curr. Opin. Plant Biol., 7, 262-269.

Kim, S.J., Jansson, S., Hoffman, N.E., Robinson, C., Mant, A. (1999) Distinct "assisted" and "spontaneous" mechanisms for the insertion of polytopic chlorophyll-binding proteins into the thylakoid membrane. J. Biol. Chem., 274, 4715-4721.

Kim, S.J., Robinson, C. and Mant A. (1998) Sec/SRP-independent insertion of two thylakoid membrane proteins bearing cleavable signal peptides. FEBS Lett. 424, 105-108.

Kleerebezem, M., Crielaard, W. and Tommassen, J. (1996) Involvement of stress protein PspA (phage shock protein A) of Escherichia coli in maintenance of the protonmotive force under stress conditions. EMBO J., 15, 162-171.

Kleerebezem, M. and Tommassen, J. (1993) Expression of the pspA gene stimulates efficient protein export in Escherichia coli. Mol Microbiol., 7, 947-956.

Klughammer, C. and Schreiber, U. (1993) Selective interaction of valinomycin/K+ with the cytochrome bf complex of chloroplasts. Synergistic effect with MOA stilbene on extent of cytochrome b563 reduction in continuous light. FEBS Lett., 336, 491-495.

Kobayashi, H., Yamamoto, M. and Aono, R. (1998) Appearance of a stress-response protein, phage-shock protein A, in *Escherichia coli* exposed to hydrophobic organic solvents. Microbiology, 144, 353-359.

Koop, H.U., Steinmuller, K., Wagner, H., Rossler, C., Eibl, C., Sacher, L. (1996) Integration of foreign sequences into the tobacco plastome via polyethylene glycol-mediated protoplast transformation. Planta, 199, 193–201.

Krause, G.H. and Weis, E. (1991) Chlorophyll Fluorescence and Photosynthesis - the Basics. Annual Review of Plant Physiology and Plant Molecular Biology, 42, 313-349.

Kroll, D., Meierhoff, K., Bechtold, N., Kinoshita, M., Westphal, S., Vothknecht, U.C., Soll, J. and Westhoff, P. (2001) VIPP1, a nuclear gene of Arabidopsis thaliana essential for thylakoid membrane formation. Proc. Natl. Acad. Sci. USA, 98, 4238-4242.

Kuchler, M., Decker, S., Hormann, F., Soll, J., Heins, L. (2002) Protein import into chloroplasts involves redox-regulated proteins. EMBO J., 21, 6136-6145.

Laemmli, U.K. (1970) Cleavage of structural proteins during the assembly of the head of bacteriophage T4. Nature, 227, 680-685.

Li, H.M., Kaneko, Y. and Keegstra, K. (1994) Molecular cloning of a chloroplastic protein associated with both the envelope and thylakoid membranes. Plant Mol. Biol., 25, 619-632.

Liu, C., Willmund, F., Whitelegge, J.P., Hawat, S., Knapp, B., Lodha, M., Schroda, M. (2005) J-domain protein CDJ2 and HSP70B are a plastidic chaperone pair that interacts wih vesicle-inducing protein in plastids 1. Mol. Biol. Cell, 16, 1165-1177.

Lloyd, L.J., Jones, S.E., Jovanovic, G., Gyaneshwar, P., Rolfe, M.D., Thompson, A., Hinton, J.C., Buck, M. (2004) Identification of a new member of the phage shock protein response in Escherichia coli, the phage shock protein G (PspG). J Biol Chem., 279, 55707-55714.

Mant, A. and Robinson, C. (2005) Biogenesis of the thylakoid membrane. Annu Plant Rev., 12, 180-213.

Margulis, L. (1970) Origin of eukaryotic cells. Yale University Press, New Haven, CT, USA

Martin, W., Stoebe, B., Goremykin, V., Hapsmann, S., Hasegawa, M., Kowalik, K.V. (1998) Gene transfer to the nucleus and the evolution of chloroplasts. Nature, 393, 162-165.

Michl, D., Robinson, C., Shackleton, J.B., Herrmann, R.G., Klösgen, R.B. (1994) Targeting of proteins to the thylakoids by bipartite presequences: CFoII is imported by a novel, third pathway EMBO J., 13, 1310-1317.

Mollier, P., Hoffmann, B., Debast, C., Small, I. (2002) The gene encoding Arabidopsis thaliana mitochondrial ribosomal protein S13 is a recent duplication of the gene encoding plastid S13. Curr. Genet., 40, 405-409.

Moreira, D., Le Guyader, H. Philippe, H. (2000) The origin of red algae and the evolution of chloroplasts. Nature, 405, 69-72.

Muehletaler, K. and Frey-Wyssing, A. (1959) Development and structure of proplastids. J. Biophys. Biochem. Cytol. 6, 507-512.

Muller, P., Li, X.P. and Niyogi, K.K. (2001) Non-photochemical quenching. A response to excess light energy. Plant Physiol., 125, 1558-1566.

Murashige, T. and Skoog, F.A. (1962) A revised medium for rapid growth and bioassays with tobacco tissue cultures. Physiol. Plant, 15, 473-497.

Ono, T. and Murata, N. (1981) Chilling susceptibility of the blue-green alga Anacystis nidulans: effect of growth temperature. Plant Physiol., 67, 176-182.

Ossenbühl, F., Gohre, V., Meurer, J., Krieger-Liszkay, A., Rochaix, J.D., Eichacker, L.A. (2004) Efficient assembly of photosystem II in Chlamydomonas reinhardtii requires Alb3.1p, a homolog of Arabidopsis ALBINO3. Plant Cell, 16, 1790-1800.

Palmer, J.D. (2000) A single birth of all plastids? Nature, 405, 32-33.

Pfannschmidt, T., Schütze, K., Brost, M., Oelmüller, R. (2001) A novel mechanism of nuclear photosynthesis gene regulation by redox signals from the chloroplast during photosystem stoichiometry adjustment. J. Biol. Chem., 276, 36125–36130.

Saiki, R.K., Gelfand, D.H., Stoffel, B., Scharf, S.J., Higuchi, R., Horn, G.T., Mullis, K.B., Ehrlich, H.A. (1998) Primer-directed enzymatic amplification of DANN with a thermo stable DANN polymerase. Science 239, 487-491.

Sambrook, J., Fritsch, E.F. and Maniatis, T. (1989) Molecular Cloning – A laboratory manual. Second Edition. Cold Spring Habor Laboratory Press, New York.

Schägger, H. and von Jagow, G. (1991) Blue native electrophoresis for isolation of membrane protein complexes in enzymatically active form. Anal. Biochem., 199, 223–231.

Sherameti, I., Shahollari, B., Landsberger, M., Westermann, M., Cherepneva, G., Kusnetsov, V., Oelmüller, R. (2004) Cytokinin stimulates polyribosome loading of nuclear-encoded mRNAs for the plastid ATP synthase in etioplasts of *Lupinus luteus*: the complex accumulates in the inner-envelope membrane with the CF_1 moiety located towards the stromal space. The Plant Journal, 38, 578-593.

Simidjiev, I., Stoylova, S., Amenitsch, H., Javorfi, T., Mustardy, L., Laggner, P., Holzenburg, A., Garab, G. (2000) Self-assembly of large, ordered lamellae from non-bilayer lipids and integral membrane proteins in vitro. Proc Natl Acad Sci USA, 97, 1473-1476.

Spurr, A.R. (1969) A low-viscosity epoxy resin embedding medium for electron microscopy. J. Ultrastruct. Res., 26, 31-43.

Stefansson, H., Andreasson, E., Weibull, C., Albertsson, P-A. (1997) Fractionation of the thylakoid membrane from *Dunaliella salina* – heterogeneity is found in Photosystem I over a broad range of growth irradiance Biochim., Biophys., Acta, 1320, 235-246.

Stein, B. (2004) Molekularbiologische und biochemische Analyse des plastidären Tetratricopeptid-Repeat-Proteins HCF107 aus *Arabidopsis thaliana*. PhD thesis.

Towbin, H., Staehlin, T. and Gordon, J. (1979) Electrophoretic transfer of proteins from polyacrylamid gels to nitrocellulose sheets: procedure and some application. Proc. Natl. Acad. Sci. USA, 76, 4350-4354.

Trissl, H-W. and Wilheim, C. (1993) Why do thylakoid membranes from higher plants form grana stacks? Trends Biochem. Sci. 18, 415–419.

Vallon, O., Bulte, L., Dainese, P., Olive, J., Bassi, R., Wollman, F.A. (1991) Lateral redistribution of cytochrome b6/f complexes along thylakoid membranes upon state transitions. Proc Natl Acad Sci USA, 88, 8262-8266.

van Kooten, O. and Snel, J.F.H. (1990) The use of chlorophyll fluorescence nomenclature in plant stress physiology. Photosynthesis Research, 25, 147-150.

van der Laan, M., Bechtluft, P., Kol, S., Nouwen, N., Driessen, A.J.M. (2004) F_1F_0 ATP synthase subunit c is a substrate of the novel YidC pathway for membrane protein biogenesis. JCB, 165, 213-222.

van der Laan, M., Urbanus, M.L., Ten Hagen-Jongman, C.M., Nouwen, N., Oudega, B., Harms, N., Driessen, A.J., Luirink, J. (2003) A conserved function of YidC in the biogenesis of respiratory chain complexes. Proc. Natl. Acad. Sci. USA, 100, 5801-5806.

van Roon, H., van Breemen, J.F.L., de Weerd, F.L., Dekker, J.P., Boekema, E.J. (2000) Solubilization of green plant thylakoid membranes with n-dodecyl-α,D-maltoside. Implications for the structural organization of the Photosystem II, Photosystem I, ATP synthase and cytochrome *b*(6)*f* complexes, Photosynth. Res., 64, 155–166.

Vothknecht, U.C. and Westhoff, P. (2001) Biogenesis and origin of thylakoid membranes. Biochim. Biophys. Acta, 1541, 91-101.

Waegemann, K. and Soll, J. (1995) Characterization and isolation of the chloroplast protein import machinery. Methods Cell Biol., 50, 255-267.

Walters, R.G. (2005) Towards an understanding of photosynthetic acclimation. J. Exp. Bot., 56, 435-447.

Weiner, L., Brissette, J.L. and Model, P. (1991) Stress-induced expression of the *Escherichia coli* phage shock protein operon is dependent on sigma 54 and modulated by positive and negative feedback mechanisms. Genes Dev., 5, 1912-1923.

Weiner, L., Brissette, J.L., Ramani, N., Model, P. (1995) Analysis of the proteins and cis-acting elements regulating the stress-induced phage shock protein operon. Nucleic Acids Res. Jun 11;23(11):2030-2036.

Weiner, L. and Model, P. (1994) Role of an *Escherichia coli* stress-response operon in stationary-phase survival. Proc. Natl. Acad. Sci. USA**,** 91, 2191-2195.

Westphal, S., Heins, L., Soll, J., Vothknecht, U.C. (2001a) Vipp1 deletion mutant of Synechocystis: a connection between bacterial phage shock and thylakoid biogenesis? Proc Natl Acad Sci USA, 98, 4243-4248.

Westphal, S., Soll, J. and Vothknecht, U.C. (2001b) A vesicle transport system inside chloroplasts. FEBS Lett. 506(3), 257-61.

Westphal, S., Soll, J. and Vothknecht, U.C. (2003) Evolution of chloroplast vesicle transport. Plant Cell Physiol., 44, 217-222.

Williams, J.G.K**.** (1988) Construction of specific mutations in photosystem II photosynthetic reaction center by genetic engineering methods in *Synechocystis* 6803. Methods Enzymol.*,* 167**,** 766-778.

Xiong, J. and Bauer, C.E. (2002) Complex evolution of photosynthesis. Annu. Rev. Plant Biol., 53, 503-521.

Xiong, F., Fischer, W.M., Inoue, K., Nakahara, M., Bauer, C.E. (2000) Molecular evidence for the early evolution of photosynthesis. Science, 289, 1724-1730.

Zak, E., Norling, B., Maitra, R., Huang, F., Andersson, B., Pakrasi, H.B. (2001) The initial steps of the biogenesis of cyanobacterial photosystems occur in plasma membranes. Proc. Natl. Acad. Sci. USA, 98, 13443–13448.

9. Publications

Publications related to this work

1. Aseeva, E., Ossenbuhl, F., Eichacker, L.A., Wanner, G., Soll, J., Vothknecht, U.C. (2004) Complex formation of Vipp1 depends on its alpha-helical PspA-like domain. J Biol Chem. 279: 35535-35541.

2. Aseeva, E., Ossenbuhl, F., Eichacker, L.A., Sippel, C., Wanner, G., Westhoff, P., Soll, J., Vothknecht, U.C. Vipp1 is required for thylakoid membrane biogenesis but not for the assembly of functional thylakoid membranes (submitted).

Other publications and publications in meeting proceedings

1. Voronin, A., Aseeva, E., Kinev, A., Margulis, B. The exogenous HSP70/HSC70 decreases DNA synthesis in human leukemia U937 cells (1995) Biology of Molecular Chaperones, Abstr. of ESF and Euroconferences Meeting, Crete (Greece). P.102.

2. Polianskaia, G.G., Kinev, A.V., Sakuta, G.A., Aseeva, E.V. (1997) Effect of an extracellular heat shock protein on chromosome variability in Indian muntjak cultured skin fibroblasts. Tsitologiia, 39(11):1070-1082.

3. Aseeva, E.V., Bulatova, M.M., Demidov, O.N., Margulis, B.A., Fridlyanskaya, I.I. Heat shock proteins expression in neuroblastoma cells SC-N-MC (Thesis) (1999) Cytologia, Vol.41.N 3-4.

Acknowledgments

I would also like to thank all members of the lab, since each of them helped me during my PhD work one way or another. Thank you for innumerous little favours, advises, questions, going outs and just for the fun that we had together.

Curriculum vitae

Date and place of birth   29 June 1972, St.-Petersburg, Russia

School education

<u>1979-1989</u>

Secondary school No. 10, St.-Petersburg, Russia

Academic education and experience

<u>1989-1996</u>

Study at the St.-Petersburg State University, Department of Genetics

<u>1995-1996</u>

Diploma degree research „Influence of the major heat shock protein (hsp70) on the proliferation and DNA synthesis of transformed immune cells". Graduated in July, 1996

<u>1996-2000</u>

Work in the Institute of Cytology of Russian Academy of Science, Department of Cell Cultures, Laboratory of Cell Protection Mechanisms. Research in the field of apoptosis in normal and tumour cells, the role of hsp70 in cytoprotection mechanisms

<u>2000 - 2002</u>

PhD thesis in the lab of Prof. Jürgen Soll at the Department of Botany at Christian-Albrechts University, Kiel

<u>2002 -</u>

Continuation of the PhD thesis at the Department of Botany at the Ludwig-Maximilians University, Munich.

Ehrenwörtliche Versicherung

Die vorliegende Dissertation wurde von Dipl. Biol. Elena Aseeva selbständig und ohne unerlaubte Hilfe angefertigt. Die Autorin hat zuvor nicht versucht, anderweitig eine Dissertation einzureichen oder sich einer Doktorprüfung zu unterziehen. Die Dissertation wurde keiner weiteren Prüfungskommission weder in Teilen noch als Ganzes vorgelegt.

Elena Aseeva,

München, den 14.11.2005